

Constraining New Physics with PVDIS

Sonny Mantry

University of North Georgia (UNG)

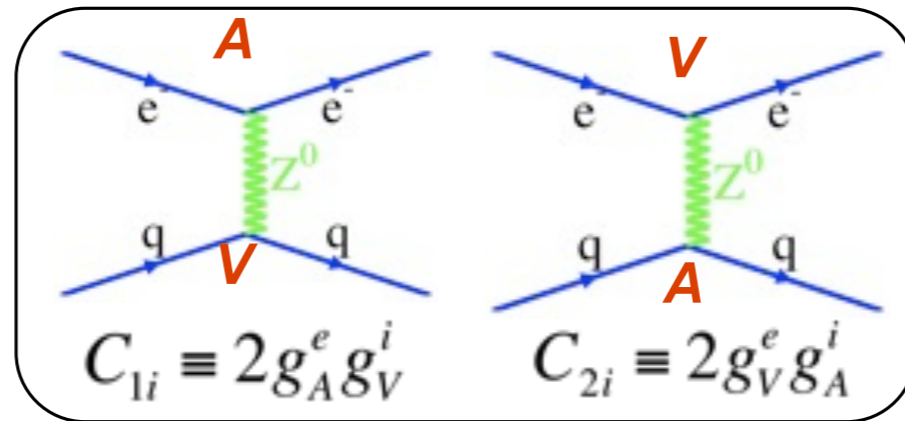
*Physics Beyond the Standard Model
High Energy Workshop Series*

*Jefferson Lab
August 1st, 2022*

Outline

- The C_{iq} couplings
- SMEFT Analysis
- Dark Photons
- Dark-Z
- Charged Lepton Violation ($e \rightarrow \mu$)

Contact Interactions



- For $Q^2 \ll (M_Z)^2$ limit, electron-quark scattering via the weak neutral current is mediated by contact interactions:

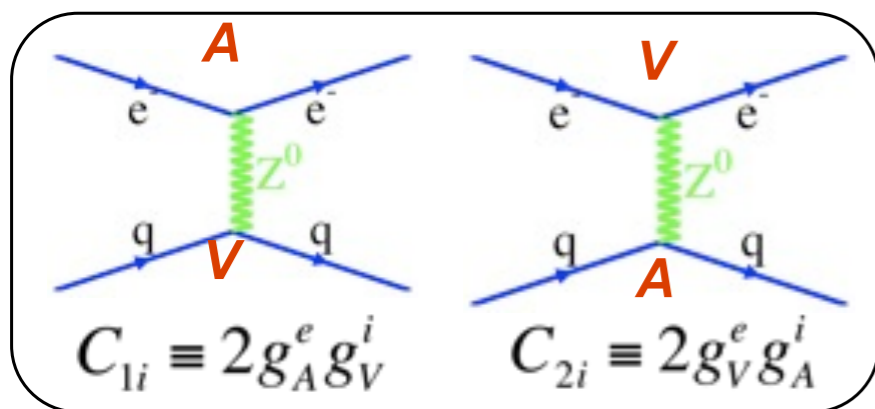
$$\mathcal{L} = \frac{G_F}{\sqrt{2}} \sum_q \left[C_{1q} \bar{\ell} \gamma^\mu \gamma_5 \ell \bar{q} \gamma_\mu q + C_{2q} \bar{\ell} \gamma^\mu \ell \bar{q} \gamma_\mu \gamma_5 q + C_{3q} \bar{\ell} \gamma^\mu \gamma_5 \ell \bar{q} \gamma_\mu \gamma_5 q \right]$$

- Tree-level Standard Model values:

$$C_{1u} = -\frac{1}{2} + \frac{4}{3} \sin^2(\theta_W), \quad C_{2u} = -\frac{1}{2} + 2 \sin^2(\theta_W), \quad C_{3u} = \frac{1}{2},$$

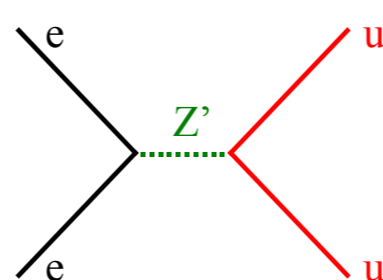
$$C_{1d} = \frac{1}{2} - \frac{2}{3} \sin^2(\theta_W), \quad C_{2d} = \frac{1}{2} - 2 \sin^2(\theta_W), \quad C_{3d} = -\frac{1}{2}$$

New Physics Effects

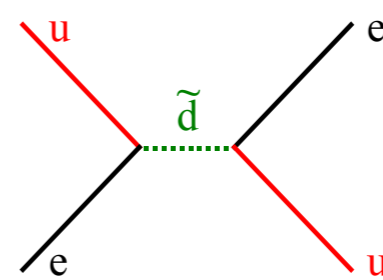


+

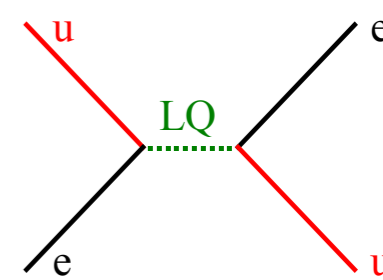
E_6 Z' Based Extensions



RPV SUSY Extensions



Leptoquarks



- In the $Q^2 \ll M_Z^2$ limit, electron-quark interactions via the weak neutral current can be parameterized by contact interactions:

$$\mathcal{L} = \frac{G_F}{\sqrt{2}} \sum_q \left[C_{1q} \bar{\ell} \gamma^\mu \gamma_5 \ell \bar{q} \gamma_\mu q + C_{2q} \bar{\ell} \gamma^\mu \ell \bar{q} \gamma_\mu \gamma_5 q + C_{3q} \bar{\ell} \gamma^\mu \gamma_5 \ell \bar{q} \gamma_\mu \gamma_5 q \right]$$

- New physics contact interactions arise as a shift in the WNC couplings compared to the SM prediction:

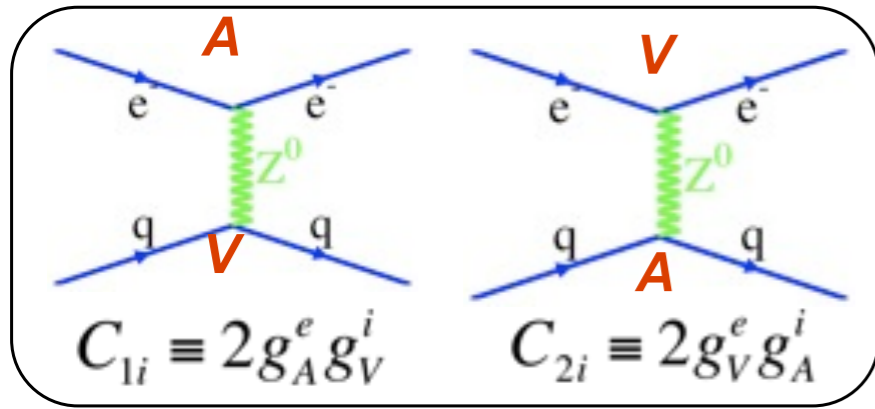
$$C_{iq} = C_{iq}(\text{SM}) + \Delta C_{iq}$$

SM contribution

New Physics contribution

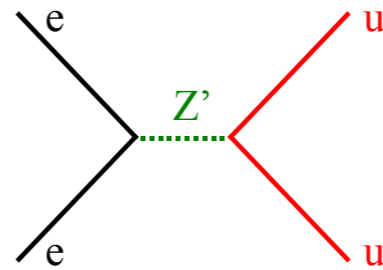
- Deviations from the SM prediction of the WNC couplings will lead to corresponding deviations in the extracted value of the weak mixing angle.

New Physics Effects

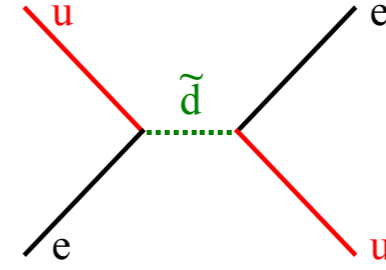


+

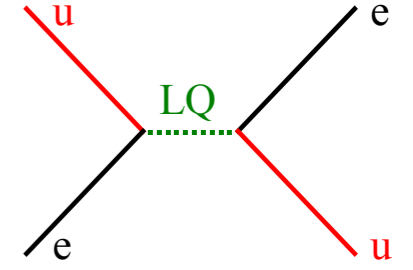
E_6 Z' Based Extensions



RPV SUSY Extensions



Leptoquarks



$$C_{iq} = C_{iq}(\text{SM}) + \Delta C_{iq}$$

- Effective Lagrangian for New Physics Contributions can be parameterized as:

$$\delta\mathcal{L} = \frac{g^2}{\Lambda^2} \sum_{\ell, q} \left\{ \eta_{LL}^{\ell q} \bar{\ell}_L \gamma_\mu \ell_L \bar{q}_L \gamma_\mu q_L + \eta_{LR}^{\ell q} \bar{\ell}_L \gamma_\mu \ell_L \bar{q}_R \gamma_\mu q_R + \eta_{RL}^{\ell q} \bar{\ell}_R \gamma_\mu \ell_R \bar{q}_L \gamma_\mu q_L + \eta_{RR}^{\ell q} \bar{\ell}_R \gamma_\mu \ell_R \bar{q}_R \gamma_\mu q_R \right\}$$

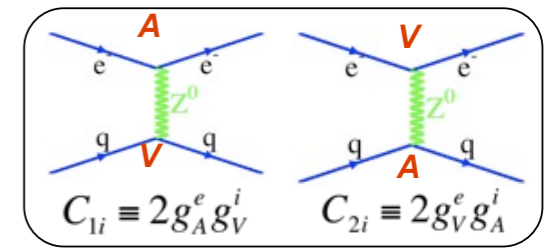
- Shift in the WNC couplings due to new physics contact interactions:

$$\Delta C_{1q} = \frac{g^2}{\Lambda^2} \frac{\eta_{LL}^{\ell q} + \eta_{LR}^{\ell q} - \eta_{RL}^{\ell q} - \eta_{RR}^{\ell q}}{2\sqrt{2}G_F},$$

$$\Delta C_{2q} = \frac{g^2}{\Lambda^2} \frac{\eta_{LL}^{\ell q} - \eta_{LR}^{\ell q} + \eta_{RL}^{\ell q} - \eta_{RR}^{\ell q}}{2\sqrt{2}G_F},$$

Each of the WNC couplings probe a unique combination of chiral structures thereby complementing constraints arising from other low energy experiments or colliders.

Contact Interactions



$$\mathcal{L} = \frac{G_F}{\sqrt{2}} \sum_q \left[C_{1q} \bar{\ell} \gamma^\mu \gamma_5 \ell \bar{q} \gamma_\mu q + C_{2q} \bar{\ell} \gamma^\mu \ell \bar{q} \gamma_\mu \gamma_5 q + C_{3q} \bar{\ell} \gamma^\mu \gamma_5 \ell \bar{q} \gamma_\mu \gamma_5 q \right]$$

- Precision measurements of the electroweak couplings can also be translated into constraints in specific models.
- For example, for the different LQ states only particular chiral structures arise which leads to a corresponding pattern of shifts in the WNC couplings:

ZEUS (prel.) 1994-2000 $e^\pm p$									
Model	Coupling structure								95% CL [TeV] M_{LQ}/λ_{LQ}
	a_{LL}^{ed}	a_{LR}^{ed}	a_{RL}^{ed}	a_{RR}^{ed}	a_{LL}^{eu}	a_{LR}^{eu}	a_{RL}^{eu}	a_{RR}^{eu}	
S_{\circlearrowleft}^L					$+\frac{1}{2}$				0.75
S_{\circlearrowright}^R								$+\frac{1}{2}$	0.69
$\tilde{S}_{\circlearrowright}^R$				$+\frac{1}{2}$					0.31
$S_{1/2}^L$						$-\frac{1}{2}$			0.91
$S_{1/2}^R$			$-\frac{1}{2}$					$-\frac{1}{2}$	0.69
$\tilde{S}_{1/2}^L$		$-\frac{1}{2}$							0.50
S_1^L	$+1$				$+\frac{1}{2}$				0.55
V_{\circlearrowleft}^L	-1								0.69
V_{\circlearrowright}^R				-1					0.58
$\tilde{V}_{\circlearrowright}^R$								-1	1.03
$V_{1/2}^L$		$+1$							0.49
$V_{1/2}^R$			$+1$				$+1$		1.15
$\tilde{V}_{1/2}^L$						$+1$			1.26
V_1^L	-1				-2				1.42

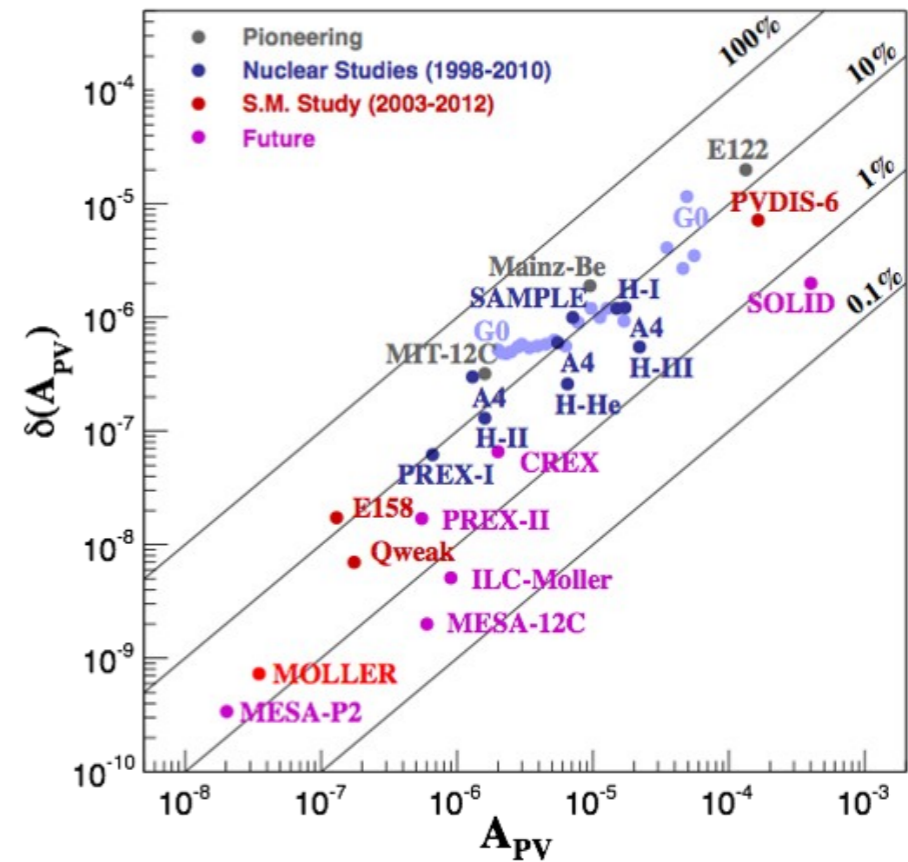
$$\Delta C_{1q} = \frac{g^2}{\Lambda^2} \frac{\eta_{LL}^{\ell q} + \eta_{LR}^{\ell q} - \eta_{RL}^{\ell q} - \eta_{RR}^{\ell q}}{2\sqrt{2}G_F},$$

$$\Delta C_{2q} = \frac{g^2}{\Lambda^2} \frac{\eta_{LL}^{\ell q} - \eta_{LR}^{\ell q} + \eta_{RL}^{\ell q} - \eta_{RR}^{\ell q}}{2\sqrt{2}G_F},$$

Accessing C_{iq} via Parity-Violating Observables

- Atomic Parity Violation (APV):
Sensitive to C_{1q} couplings via $Q_W(Z, N)$
- Parity Violating Elastic Scattering (Qweak, P2):
Sensitive to C_{1q} couplings through $Q_W(Z = 1, N = 0)$

$$Q_W(Z, N) = -2[C_{1u}(2Z + N) + C_{1d}(Z + 2N)]$$

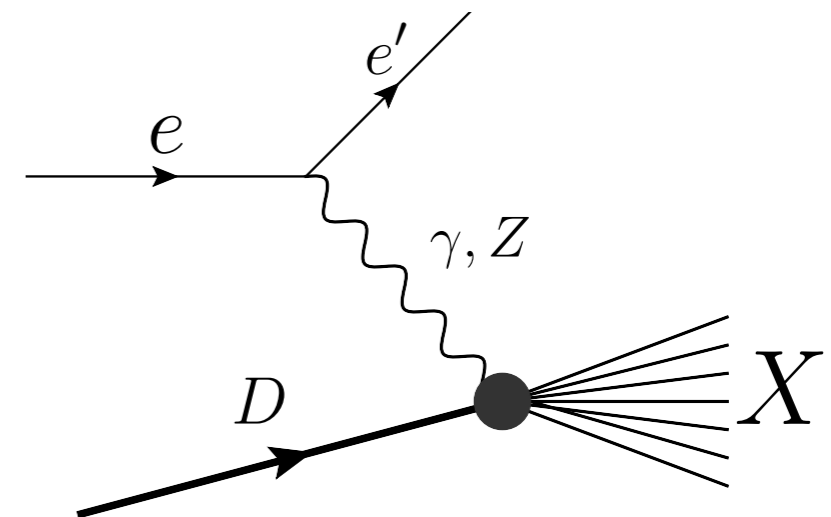


- Parity Violating DIS (E122, PVDIS-6, SOLID):
Sensitive to C_{1q} and C_{2q}

$$A_{PV}^{DIS} = \frac{G_F Q^2}{4\sqrt{2}(1 + Q^2/M_Z^2)\pi\alpha} \left[a_1 + \frac{1 - (1 - y)^2}{1 + (1 - y)^2} a_3 \right]$$

$$a_1 = \frac{2 \sum_q e_q C_{1q}(q + \bar{q})}{\sum_q e_q^2 (q + \bar{q})} \quad a_3 = \frac{2 \sum_q e_q C_{2q}(q - \bar{q})}{\sum_q e_q^2 (q + \bar{q})}$$

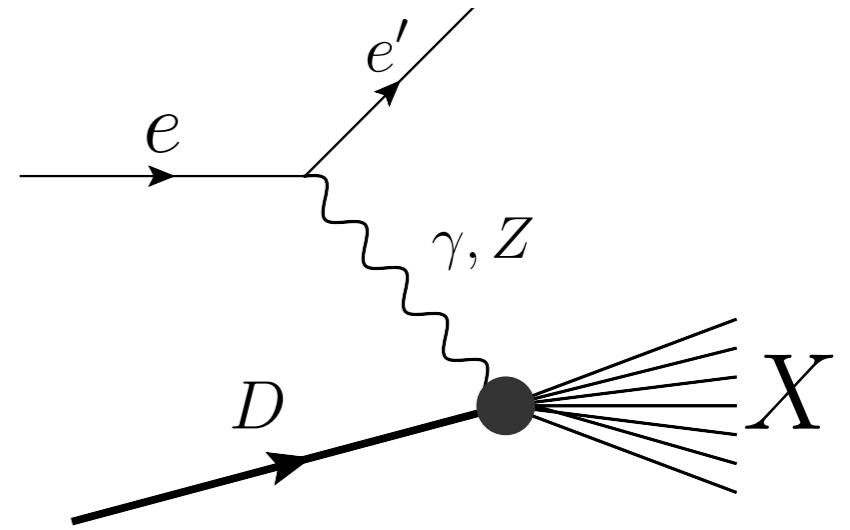
For the isoscalar deuteron target,
structure function effects largely cancel



Parity-Violating e-D Asymmetry

- Parity-violating e-D asymmetry is a powerful probe of the WNC couplings:

$$A_{\text{PV}} \equiv \frac{\sigma_R - \sigma_L}{\sigma_R + \sigma_L} \simeq \frac{|A_Z|}{|A_\gamma|} \simeq \frac{G_F Q^2}{4\pi\alpha} \simeq 10^{-4} Q^2$$



- Due to the isoscalar nature of the Deuteron target, the dependence of the asymmetry on the structure functions largely cancels (Cahn-Gilman formula).

$$A_{\text{CG}}^{\text{RL}} = -\frac{G_F Q^2}{2\sqrt{2}\pi\alpha} \frac{9}{10} \left[\left(1 - \frac{20}{9} \sin^2 \theta_W\right) + \left(1 - 4 \sin^2 \theta_W\right) \frac{1 - (1 - y)^2}{1 + (1 - y)^2} \right]$$

All hadronic effects cancel!

Clean probe of WNC

- e-D asymmetry allows a precision measurement of the weak mixing angle.

Corrections to Cahn-Gilman

- Hadronic effects appear as corrections to the Cahn-Gilman formula:

$$A_{RL} = -\frac{G_F Q^2}{2\sqrt{2}\pi\alpha} \frac{9}{10} \left[\tilde{a}_1 + \tilde{a}_2 \frac{1 - (1 - y)^2}{1 + (1 - y)^2} \right]$$

$$\tilde{a}_j = -\frac{2}{3} (2C_{ju} - C_{jd}) [1 + R_j(\text{new}) + R_j(\text{sea}) + R_j(\text{CSV}) + R_j(\text{TMC}) + R_j(\text{HT})]$$

↑
New physics

↑
Sea quarks

↑
Charge symmetry
violation

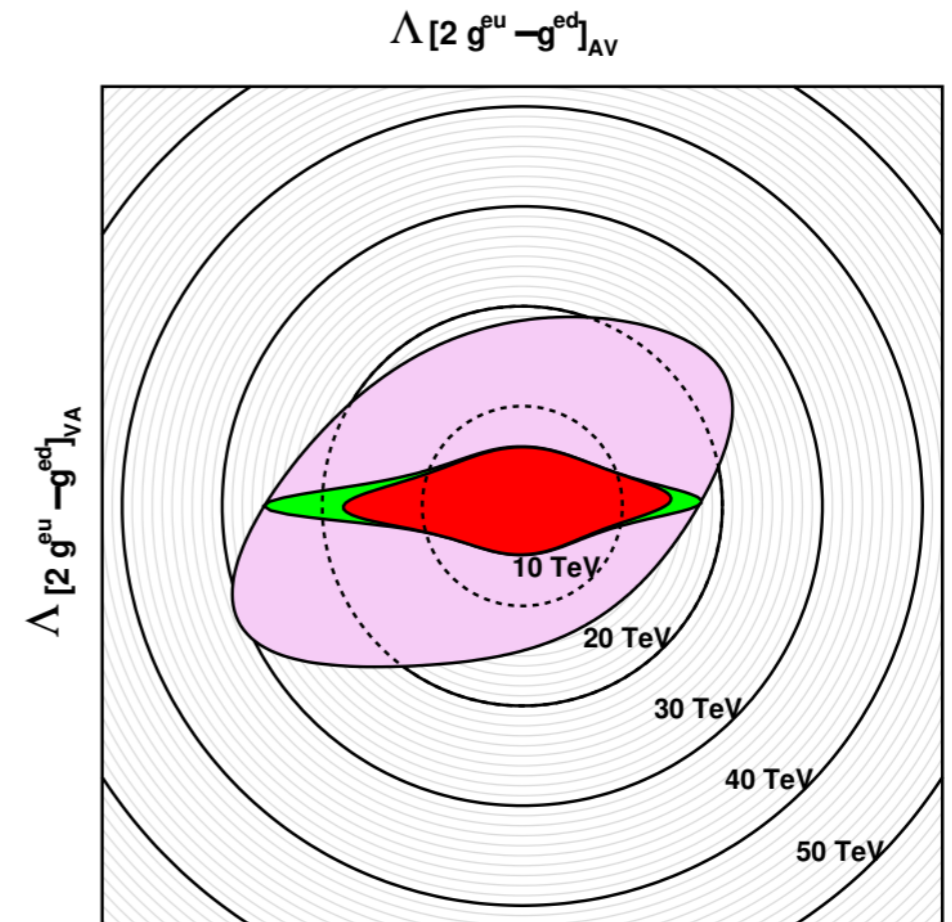
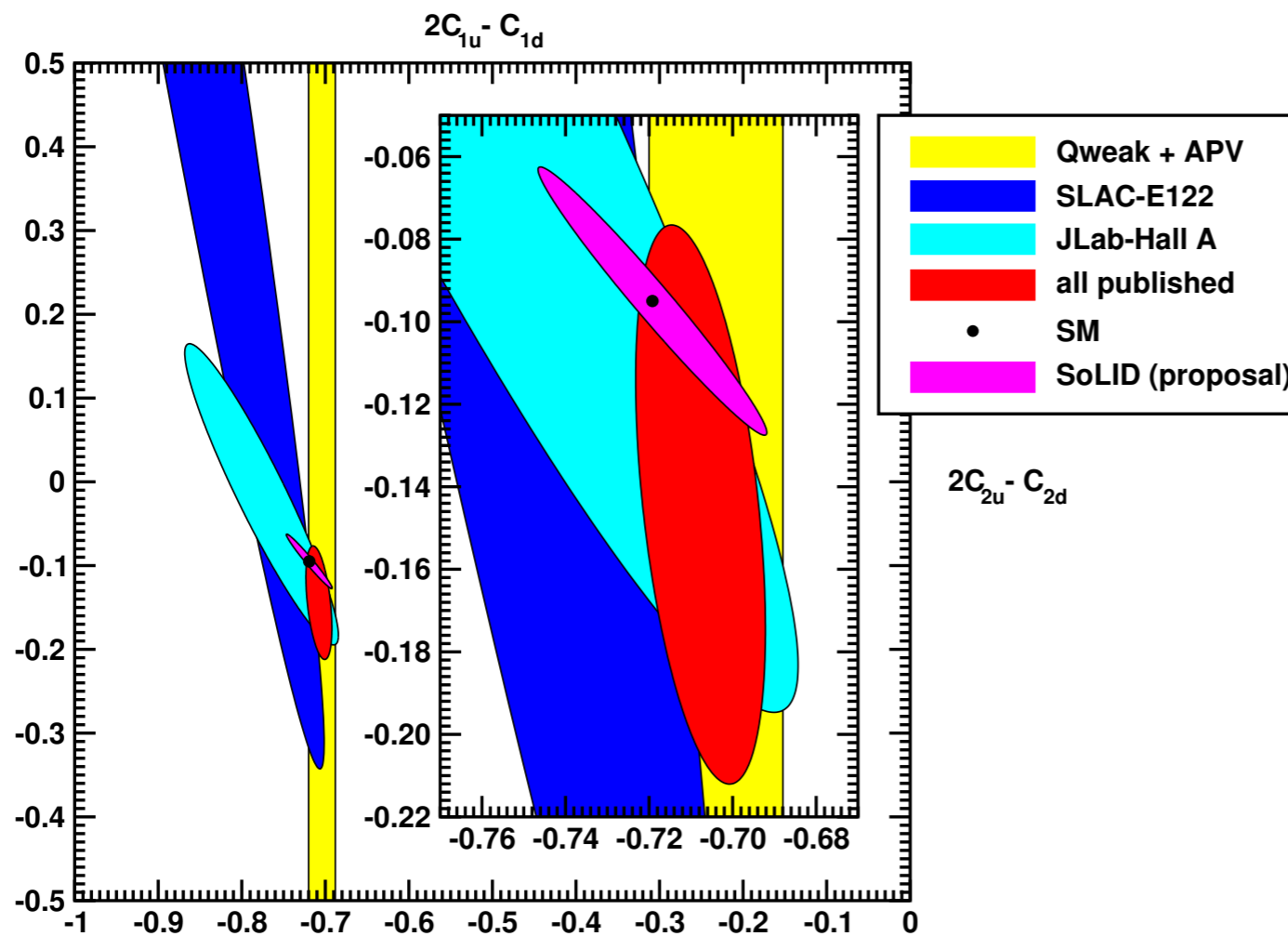
↑
Target mass

↑
Higher
twist

- Hadronic effects must be well understood before any claim for evidence of new physics can be made.

[Bjorken, Hobbs, Melnitchouk;
SM, Ramsey-Musolf, Sacco;
Belitsky, Mashanov, Schafer;
Seng, Ramsey-Musolf,]

Status of WNC Couplings



- The combination $2C_{1u} - C_{1d}$ is severely constrained by Qweak and Atomic Parity violation.
- The combination $2C_{2u} - C_{2d}$ is known to within $\sim 50\%$ from the JLAB 6 GeV experiment:

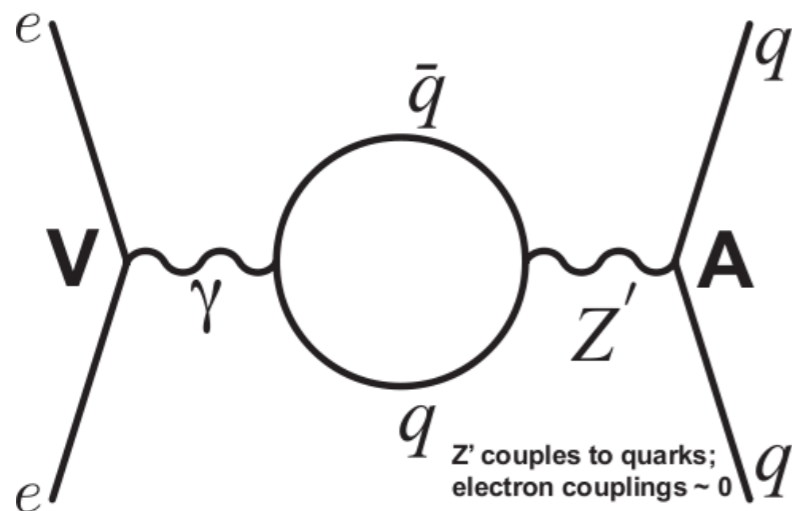
$$2C_{2u} - C_{2d} = -0.145 \pm 0.068$$

- SOLID is expected significantly improve on this result.

Leptophobic Z'

- Leptophobic Z's are an interesting BSM scenario since they only shifts the C_{2q} couplings in A_{PV}

- Leptophobic Z's only affect the $b(x)$ term or the C_{2q} coefficients in A_{PV} :

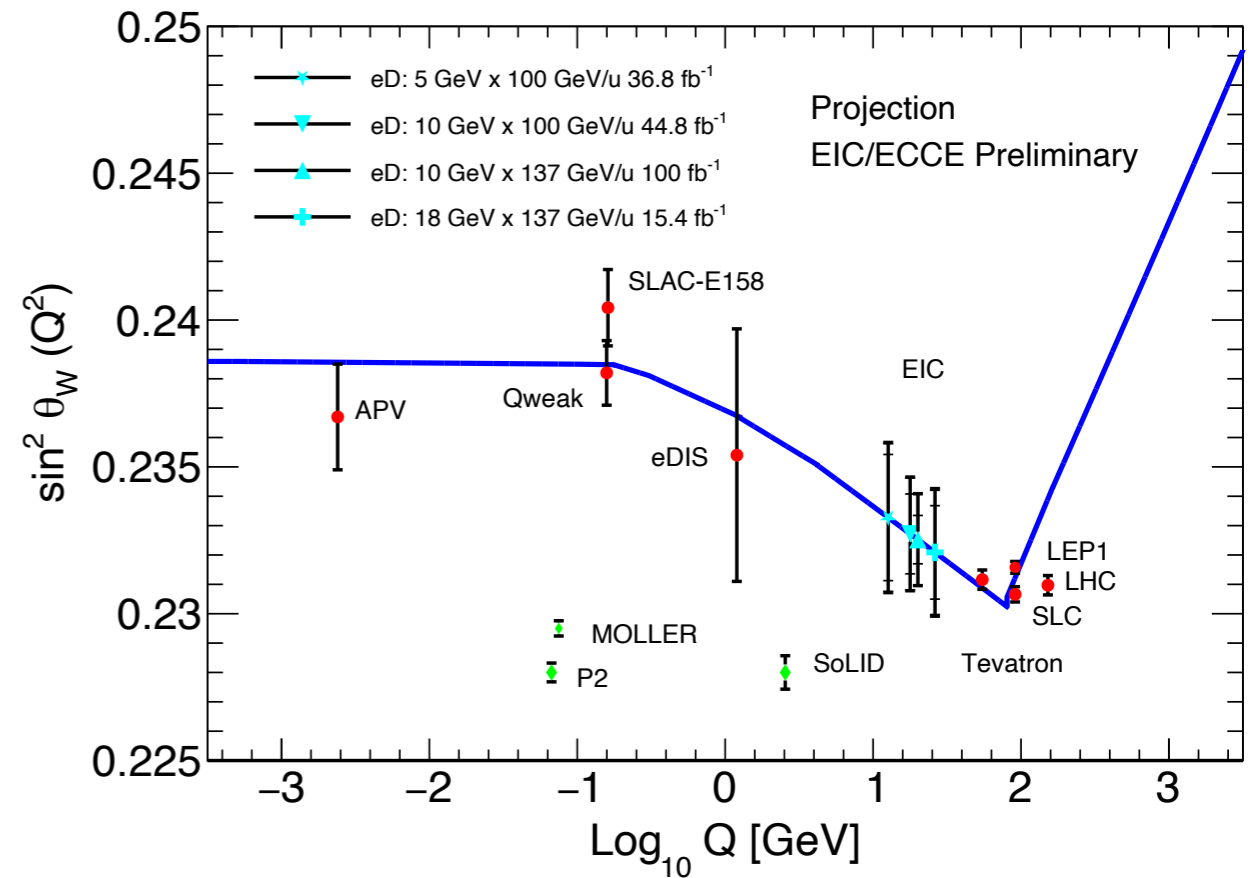
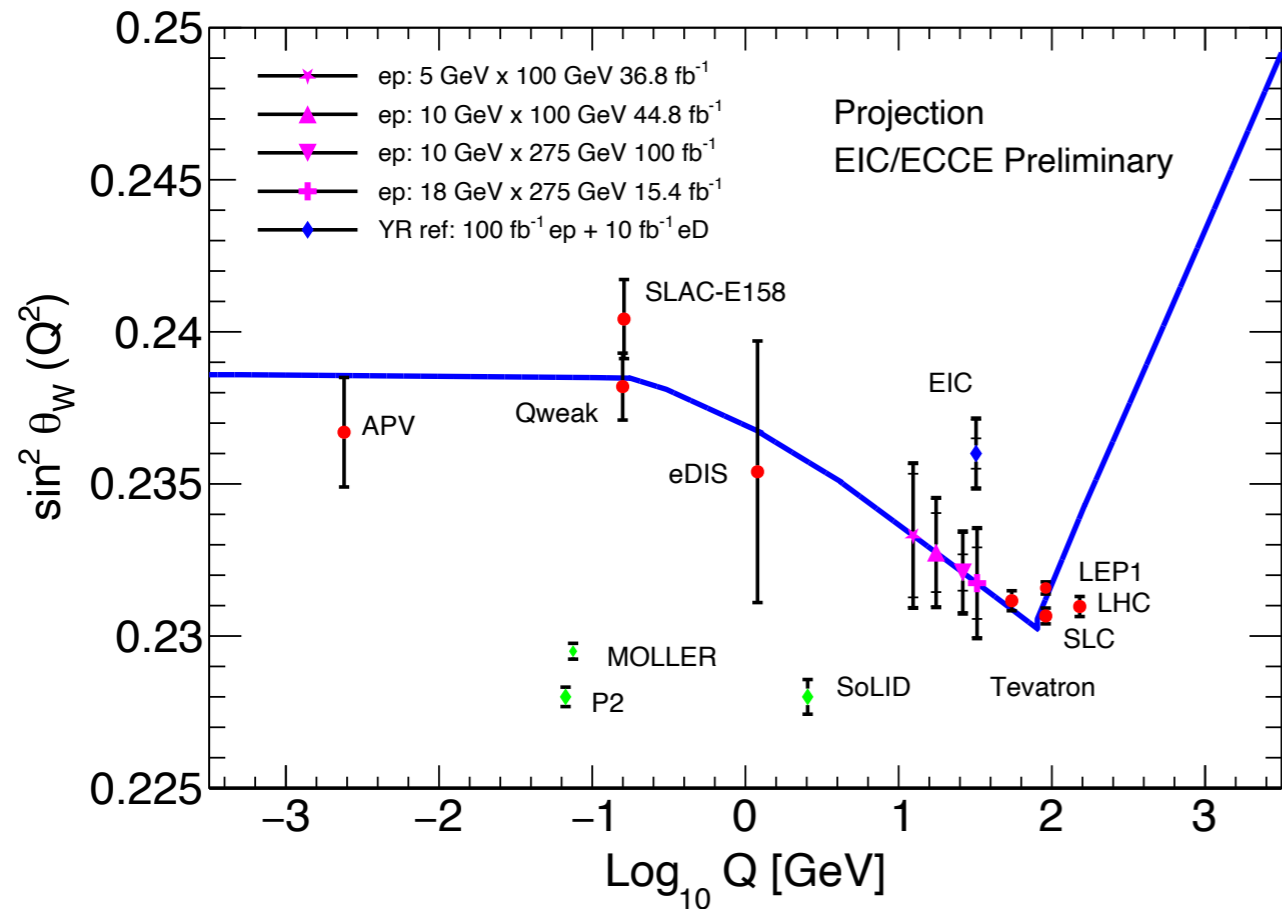


Leptophobic Z'
contributes only to
the C_{2q} couplings!

[M.Alonso-Gonzalez, M.Ramsey-Musolf;
M.Buckley, M.Ramsey-Musolf]

$$A_{PV}^{\text{DIS}} = \frac{G_F Q^2}{4\sqrt{2}(1 + Q^2/M_Z^2)\pi\alpha} \left[a_1 + \frac{1 - (1 - y)^2}{1 + (1 - y)^2} a_3 \right]$$

Extraction of the Weak Mixing Angle



[Boughazel, Emmert, Kutz, SM, Nycz, Petriello, Simsek, Wiegand, Zheng]

- SOLID is extract the weak mixing angle with higher precision than the EIC.
- How does SOLID measurement contribute in the global fit that includes data from APV, Qweak, P2, and LHC?

Standard Model Effective Theory (SMEFT)

Operator Basis

[Boughazel, Petriello, Wiegand]

- The SMEFT basis often used in global fit analysis to constrain new physics beyond the electroweak scale:

$$\mathcal{L} = \mathcal{L}_{SM} + \frac{1}{\Lambda^2} \sum_i C_i^6 \mathcal{O}_{6,i} + \frac{1}{\Lambda^4} \sum_i C_i^8 \mathcal{O}_{8,i} + \dots$$

- Relevant SMEFT operators for DIS processes at dim-6 and dim-8

Dimension 6		Dimension 8	
$\mathcal{O}_{lq}^{(1)}$	$(\bar{l}\gamma^\mu l) (\bar{q}\gamma_\mu q)$	$\mathcal{O}_{l^2 q^2 D^2}^{(1)}$	$D^\nu (\bar{l}\gamma^\mu l) D_\nu (\bar{q}\gamma_\mu q)$
$\mathcal{O}_{lq}^{(3)}$	$(\bar{l}\gamma^\mu \tau^i l) (\bar{q}\gamma_\mu \tau^i q)$	$\mathcal{O}_{l^2 q^2 D^2}^{(3)}$	$D^\nu (\bar{l}\gamma^\mu \tau^i l) D_\nu (\bar{q}\gamma_\mu \tau^i q)$
\mathcal{O}_{eu}	$(\bar{e}\gamma^\mu e) (\bar{u}\gamma_\mu u)$	$\mathcal{O}_{e^2 u^2 D^2}^{(1)}$	$D^\nu (\bar{e}\gamma^\mu e) D_\nu (\bar{u}\gamma_\mu u)$
\mathcal{O}_{ed}	$(\bar{e}\gamma^\mu e) (\bar{d}\gamma_\mu d)$	$\mathcal{O}_{e^2 d^2 D^2}^{(1)}$	$D^\nu (\bar{e}\gamma^\mu e) D_\nu (\bar{d}\gamma_\mu d)$
\mathcal{O}_{lu}	$(\bar{l}\gamma^\mu l) (\bar{u}\gamma_\mu u)$	$\mathcal{O}_{l^2 u^2 D^2}^{(1)}$	$D^\nu (\bar{l}\gamma^\mu l) D_\nu (\bar{u}\gamma_\mu u)$
\mathcal{O}_{ld}	$(\bar{l}\gamma^\mu l) (\bar{d}\gamma_\mu d)$	$\mathcal{O}_{l^2 d^2 D^2}^{(1)}$	$D^\nu (\bar{l}\gamma^\mu l) D_\nu (\bar{d}\gamma_\mu d)$
\mathcal{O}_{qe}	$(\bar{q}\gamma^\mu q) (\bar{e}\gamma_\mu e)$	$\mathcal{O}_{q^2 e^2 D^2}^{(1)}$	$D^\nu (\bar{q}\gamma^\mu q) D_\nu (\bar{e}\gamma_\mu e)$

SMEFT vs C_{iq} Basis

[Boughazel, Petriello, Wiegand]

- For low energy experiments, typically the C_{iq} basis of operators based on V-A structure after EWSB is used:

$$\begin{aligned} \mathcal{L}_{PV} = \frac{G_F}{\sqrt{2}} & \left[(\bar{e}\gamma^\mu\gamma_5 e)(C_{1u}^6 \bar{u}\gamma_\mu u + C_{1d}^6 \bar{d}\gamma_\mu d) + (\bar{e}\gamma^\mu e)(C_{2u}^6 \bar{u}\gamma_\mu\gamma_5 u + C_{2d}^6 \bar{d}\gamma_\mu\gamma_5 d) \right. \\ & + (\bar{e}\gamma^\mu e)(C_{Vu}^6 \bar{u}\gamma_\mu u + C_{Vd}^6 \bar{d}\gamma_\mu d) + (\bar{e}\gamma^\mu\gamma_5 e)(C_{Au}^6 \bar{u}\gamma_\mu\gamma_5 u) \\ & + D^\nu \left(\bar{e}\gamma^\mu\gamma_5 e \right) D_\nu \left(\frac{C_{1u}^8}{v^2} \bar{u}\gamma_\mu u + \frac{C_{1d}^8}{v^2} \bar{d}\gamma_\mu d \right) + D^\nu \left(\bar{e}\gamma^\mu e \right) D_\nu \left(\frac{C_{2u}^8}{v^2} \bar{u}\gamma_\mu\gamma_5 u + \frac{C_{2d}^8}{v^2} \bar{d}\gamma_\mu\gamma_5 d \right) \\ & \left. + D^\nu \left(\bar{e}\gamma^\mu e \right) D_\nu \left(\frac{C_{Vu}^8}{v^2} \bar{u}\gamma_\mu u + \frac{C_{Vd}^8}{v^2} \bar{d}\gamma_\mu d \right) + D^\nu \left(\bar{e}\gamma^\mu\gamma_5 e \right) D_\nu \left(\frac{C_{Au}^8}{v^2} \bar{u}\gamma_\mu\gamma_5 u \right) \right]. \end{aligned}$$

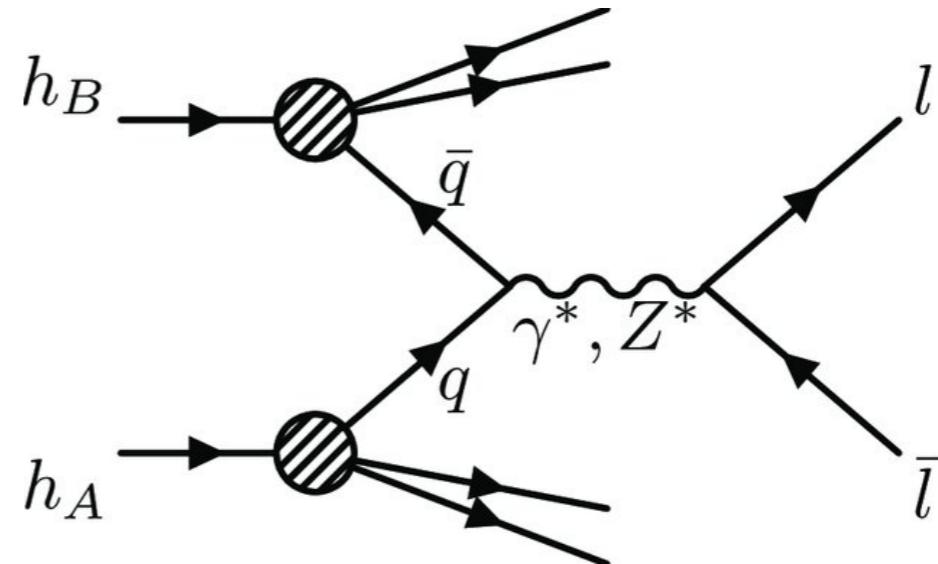
- One can find relations between the two bases:

$$\begin{aligned} C_{1u}^6 &= 2(g_R^e - g_L^e)(g_R^u + g_L^u) + \frac{v^2}{2\Lambda^2} \left\{ - \left(C_{lq}^{(1)} - C_{lq}^{(3)} \right) + C_{eu} + C_{qe} - C_{lu} \right\} \\ C_{2u}^6 &= 2(g_R^e + g_L^e)(g_R^u - g_L^u) + \frac{v^2}{2\Lambda^2} \left\{ - \left(C_{lq}^{(1)} - C_{lq}^{(3)} \right) + C_{eu} - C_{qe} + C_{lu} \right\} \\ C_{1d}^6 &= 2(g_R^e - g_L^e)(g_R^d + g_L^d) + \frac{v^2}{2\Lambda^2} \left\{ - \left(C_{lq}^{(1)} + C_{lq}^{(3)} \right) + C_{ed} + C_{qe} - C_{ld} \right\} \\ C_{2d}^6 &= 2(g_R^e + g_L^e)(g_R^d - g_L^d) + \frac{v^2}{2\Lambda^2} \left\{ - \left(C_{lq}^{(1)} + C_{lq}^{(3)} \right) + C_{ed} - C_{qe} + C_{ld} \right\} \\ C_{Vu}^6 &= 2(g_R^e + g_L^e)(g_R^u + g_L^u) + \frac{v^2}{2\Lambda^2} \left\{ \left(C_{lq}^{(1)} - C_{lq}^{(3)} \right) + C_{eu} + C_{qe} + C_{lu} \right\} \\ C_{Au}^6 &= 2(g_R^e - g_L^e)(g_R^u - g_L^u) + \frac{v^2}{2\Lambda^2} \left\{ \left(C_{lq}^{(1)} - C_{lq}^{(3)} \right) + C_{eu} - C_{qe} - C_{lu} \right\} \\ C_{Vd}^6 &= 2(g_R^e + g_L^e)(g_R^d + g_L^d) + \frac{v^2}{2\Lambda^2} \left\{ \left(C_{lq}^{(1)} + C_{lq}^{(3)} \right) + C_{ed} + C_{qe} + C_{ld} \right\}. \end{aligned}$$

SMEFT Constraints from Drell-Yan at LHC

[Boughazel, Petriello, Wiegand]

- The SMEFT Wilson coefficients that affect PVES also contribute to the Drell-Yan process at the LHC

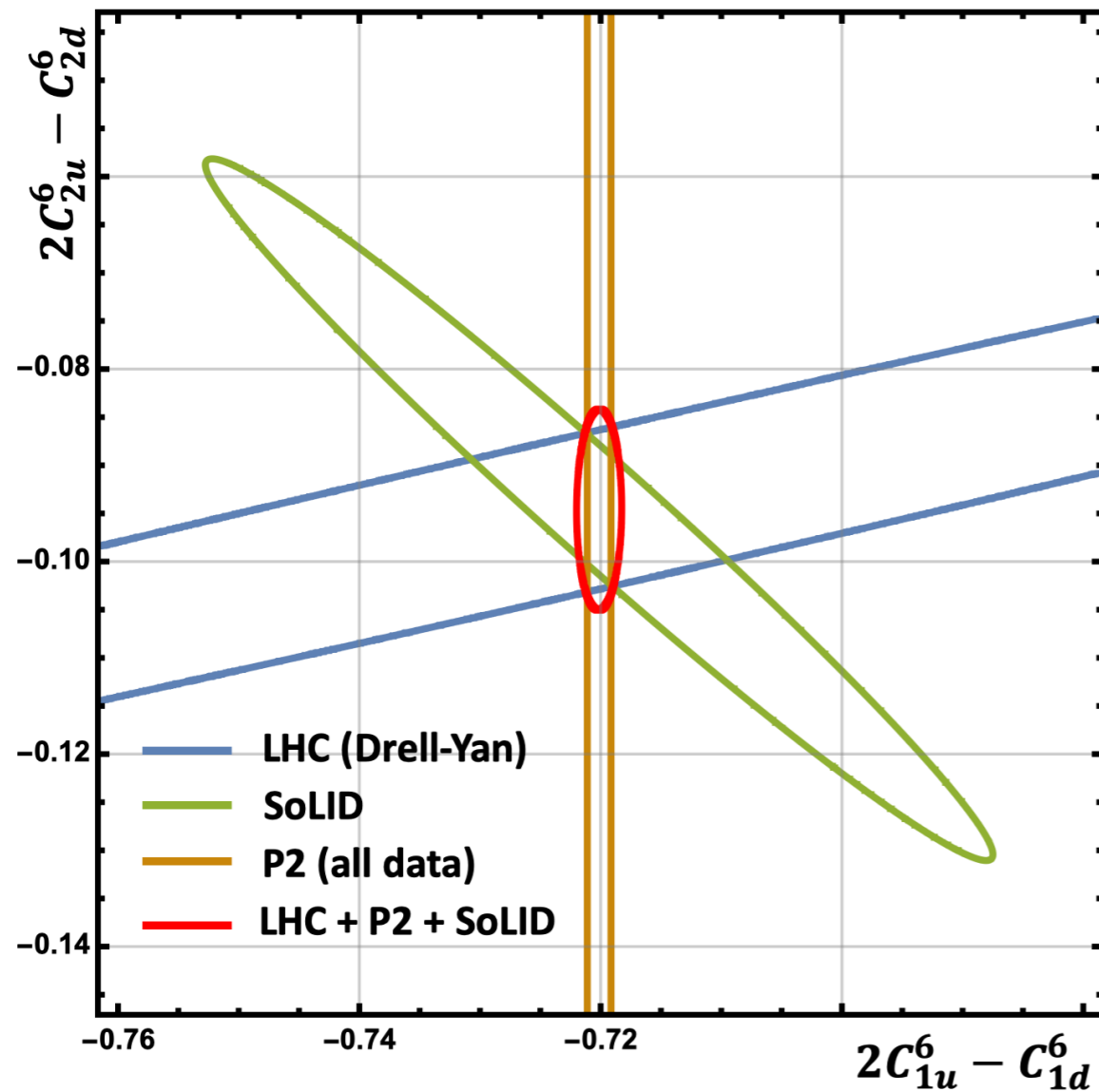


$$\frac{d\sigma_{q\bar{q}}}{dm_{ll}^2 dY dc_\theta} = \frac{1}{32\pi m_{ll}^2 \hat{s}} f_q(x_1) f_{\bar{q}}(x_2) \left\{ \frac{d\hat{\sigma}_{q\bar{q}}^{\gamma\gamma}}{dm_{ll}^2 dY dc_\theta} + \frac{d\hat{\sigma}_{q\bar{q}}^{\gamma Z}}{dm_{ll}^2 dY dc_\theta} + \frac{d\hat{\sigma}_{q\bar{q}}^{ZZ}}{dm_{ll}^2 dY dc_\theta} \right. \\ \left. + \frac{d\hat{\sigma}_{q\bar{q}}^{\gamma SMEFT6}}{dm_{ll}^2 dY dc_\theta} + \frac{d\hat{\sigma}_{q\bar{q}}^{Z SMEFT6}}{dm_{ll}^2 dY dc_\theta} + \frac{d\hat{\sigma}_{q\bar{q}}^{\gamma SMEFT8}}{dm_{ll}^2 dY dc_\theta} + \frac{d\hat{\sigma}_{q\bar{q}}^{Z SMEFT8}}{dm_{ll}^2 dY dc_\theta} + \frac{d\hat{\sigma}_{q\bar{q}}^{SMEFT6^2}}{dm_{ll}^2 dY dc_\theta} \right\}$$

- PVES and the LHC can be complementary to each other in constraining new physics

Lifting Flat Directions

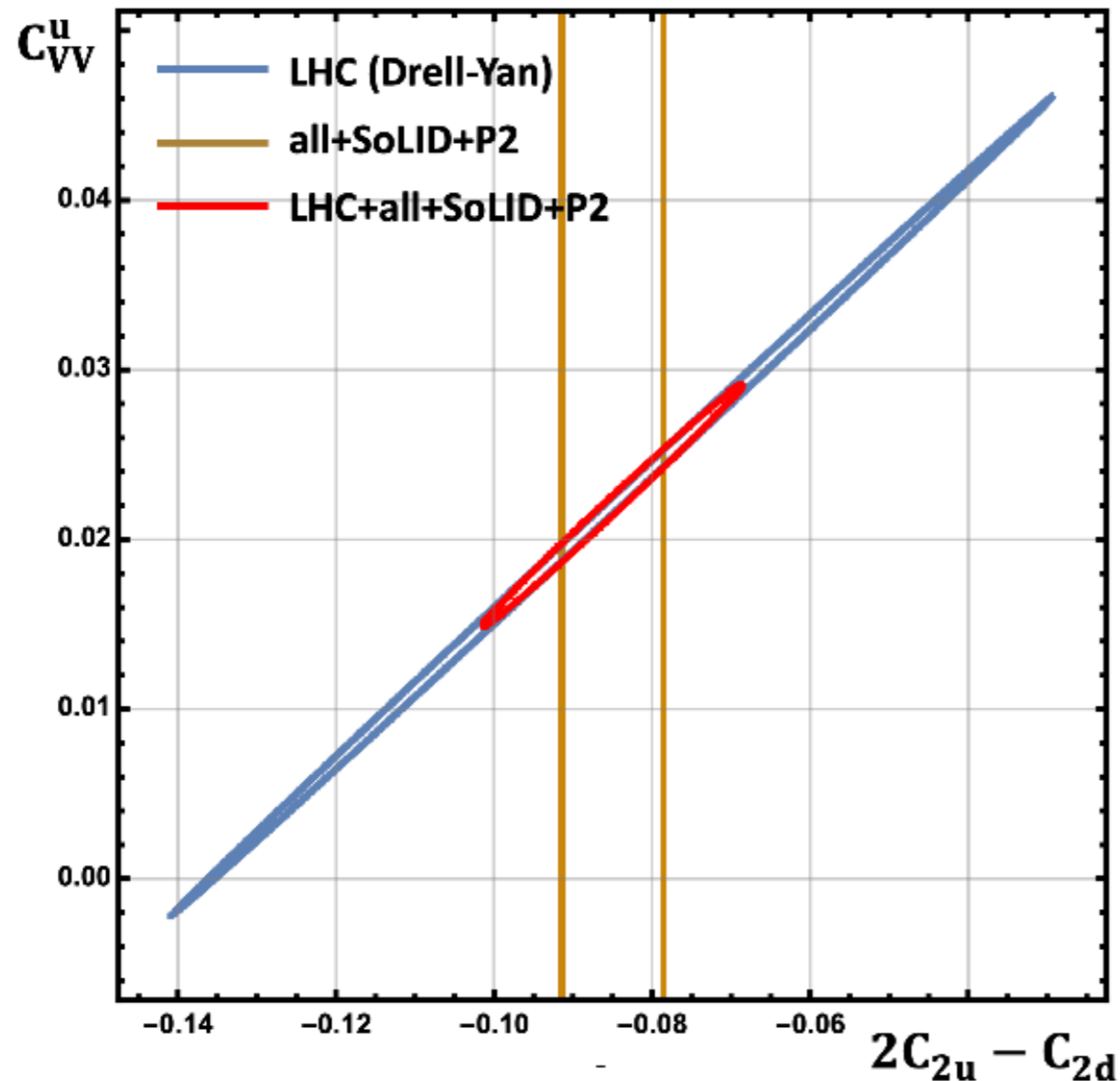
[Boughazel, Petriello, Wiegand]



- PVES and Drell-Yan at the LHC are sensitive to different combinations of the SMEFT Wilson coefficients.
- PVES can lift “flat directions” by probing orthogonal directions in the SMEFT parameter space compared to the LHC

Lifting Flat Directions

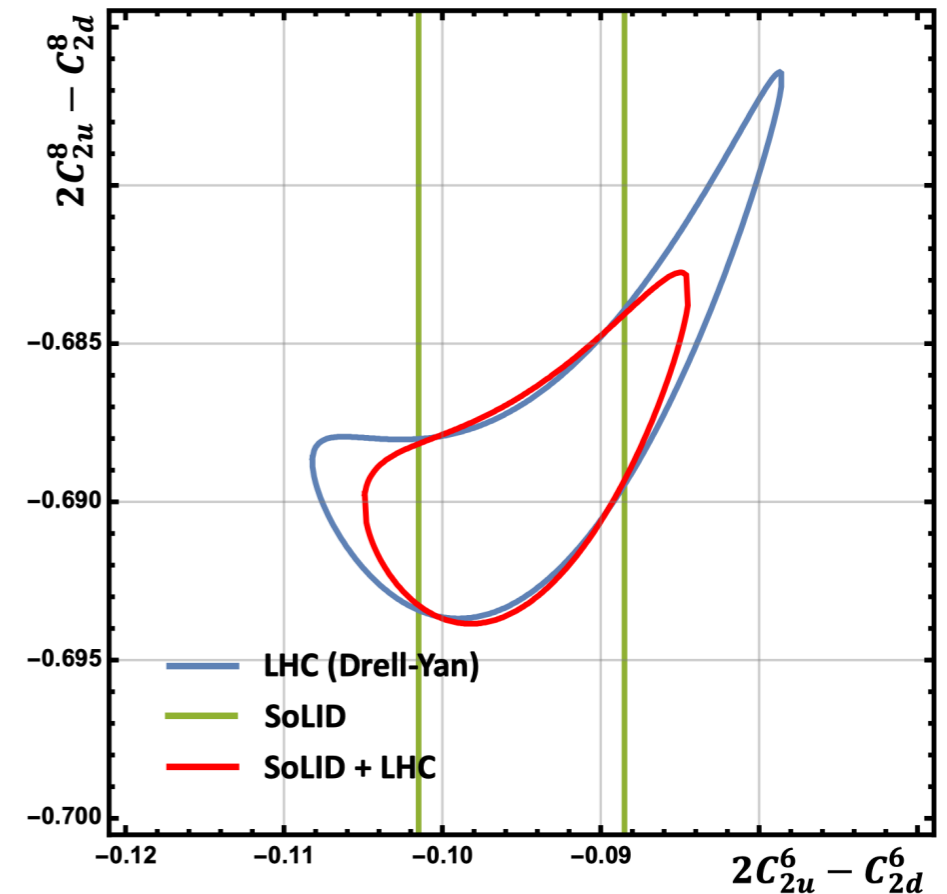
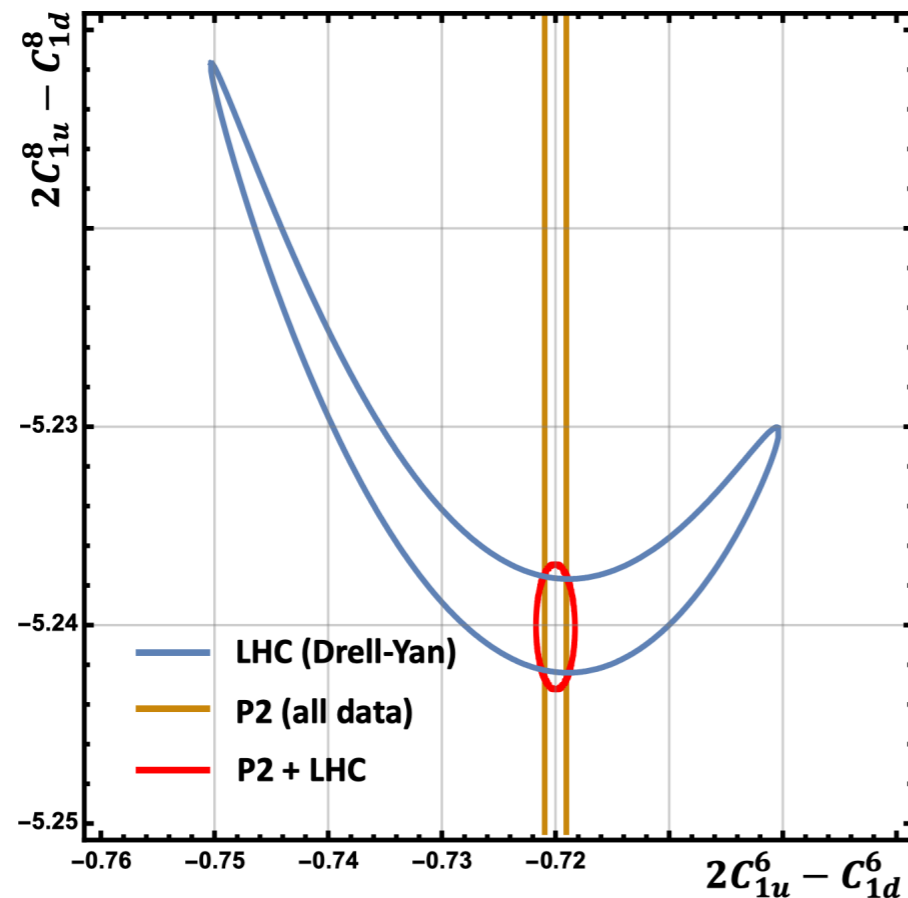
[Boughazel, Petriello, Wiegand]



- An example of SOLID probing a unique direction in parameter space. Neither the LHC, Qweak, P2, or APV have sensitivity in this region
- This requires that $2C_{1u} - C_{1d}$ is assumed to be known from the P2 experiment so that the SOLID then directly measures $2C_{2u} - C_{2d}$

Disentangling Dim-6 and Dim-8 SMEFT Operators

[Boughazel, Petriello, Wiegand]



- Another advantage of low energy PVES experiments:

The large energy of the LHC can make it difficult to disentangle the effects of dim-6 or dim-8 (and dim-6 squared) operators.

Low energy PVES will only have sensitivity to dim-6 operators providing valuable input to disentangle dim-6 vs dim-8.

Accessing C_{3q} via Parity-Violating Observables

- The C_{3q} couplings are parity conserving but can be accessed by comparing DIS cross sections with unpolarized or polarized leptons and anti-leptons

$$A^{e^+e^-} \equiv \frac{\sigma^{e^+} - \sigma^{e^-}}{\sigma^{e^+} + \sigma^{e^-}} \quad A_{ij}^{e^+e^-} \equiv \frac{\sigma_i^{e^+} - \sigma_j^{e^-}}{\sigma_i^{e^+} + \sigma_j^{e^-}} \quad (i, j = R, L)$$

- The combination of C_{3q} couplings are poorly known; have only been measured using polarized muon and anti-muon beams incident on a Carbon target:

[Erler, Ramsey-Musolf, Prog. Part. Nucl. Phys. 54, 351, (2005)]

Beam	Process	$\overline{Q^2}$ [GeV ²]	Combination	Result/Status	SM
SLAC	e^- -D DIS	1.39	$2C_{1u} - C_{1d}$	-0.90 ± 0.17	-0.7185
SLAC	e^- -D DIS	1.39	$2C_{2u} - C_{2d}$	$+0.62 \pm 0.81$	-0.0983
CERN	μ^\pm -C DIS	34	$0.66(2C_{2u} - C_{2d}) + 2C_{3u} - C_{3d}$	$+1.80 \pm 0.83$	+1.4351
CERN	μ^\pm -C DIS	66	$0.81(2C_{2u} - C_{2d}) + 2C_{3u} - C_{3d}$	$+1.53 \pm 0.45$	+1.4204
Mainz	e^- -Be QE	0.20	$2.68C_{1u} - 0.64C_{1d} + 2.16C_{2u} - 2.00C_{2d}$	-0.94 ± 0.21	-0.8544
Bates	e^- -C elastic	0.0225	$C_{1u} + C_{1d}$	0.138 ± 0.034	+0.1528
Bates	e^- -D QE	0.1	$C_{2u} - C_{2d}$	0.015 ± 0.042	-0.0624
JLAB	e^- -p elastic	0.03	$2C_{1u} + C_{1d}$	approved	+0.0357
SLAC	e^- -D DIS	20	$2C_{1u} - C_{1d}$	to be proposed	-0.7185
SLAC	e^- -D DIS	20	$2C_{2u} - C_{2d}$	to be proposed	-0.0983
SLAC	e^\pm -D DIS	20	$2C_{3u} - C_{3d}$	to be proposed	+1.5000
—	¹³³ Cs APV	0	$-376C_{1u} - 422C_{1d}$	-72.69 ± 0.48	-73.16
—	²⁰⁵ Tl APV	0	$-572C_{1u} - 658C_{1d}$	-116.6 ± 3.7	-116.8

$$2g_{AA}^{\mu u} - g_{AA}^{\mu d} + 0.81(2g_{VA}^{\mu u} - g_{VA}^{\mu d}) = 1.45 \pm 0.41$$

$$2g_{AA}^{\mu u} - g_{AA}^{\mu d} + 0.66(2g_{VA}^{\mu u} - g_{VA}^{\mu d}) = 1.70 \pm 0.79$$



Using PVDIS 6 GeV

$$2g_{AA}^{\mu u} - g_{AA}^{\mu d} = 1.57 \pm 0.38.$$

[Erler, Liu, Spiesberger, Zheng]

Probing the Dark Sector

- Strong evidence for dark matter through gravitational effects:

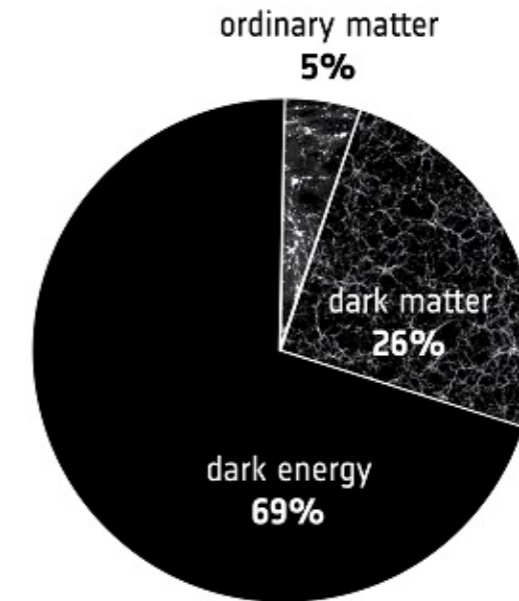
- Galactic Rotation Curves
- Gravitational Lensing
- Cosmic Microwave Background
- Large Scale Structure Surveys

- WIMP dark matter paradigm

- Mass \sim TeV
- Weak interaction strength couplings
- Gives the required relic abundance

- However, so far no direct evidence for WIMP dark matter

- Perhaps dark sector has a rich structure including different species and gauge forces, just like the visible sector



Dark Photon Scenario

- Dark $U(1)_d$ gauge group
- Interacts with SM via kinetic mixing (and mass mixing)

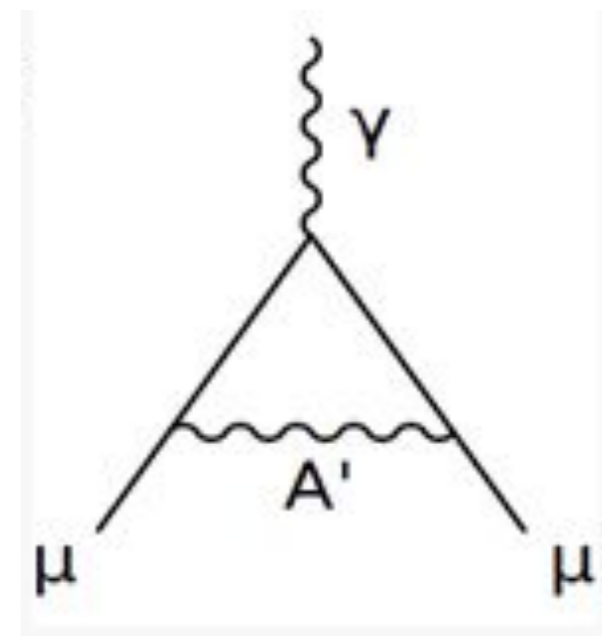
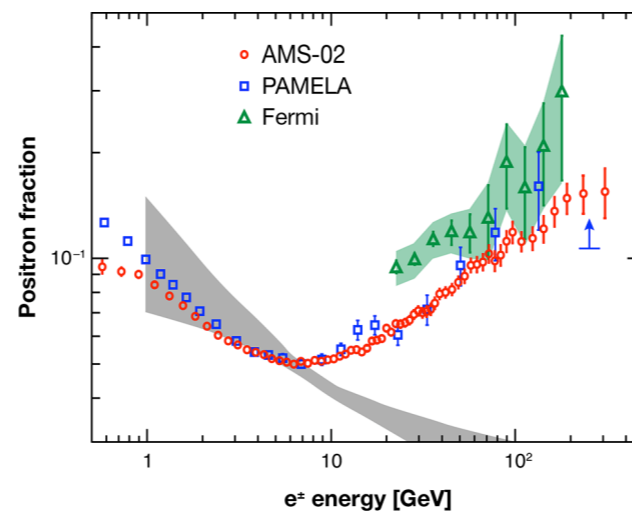
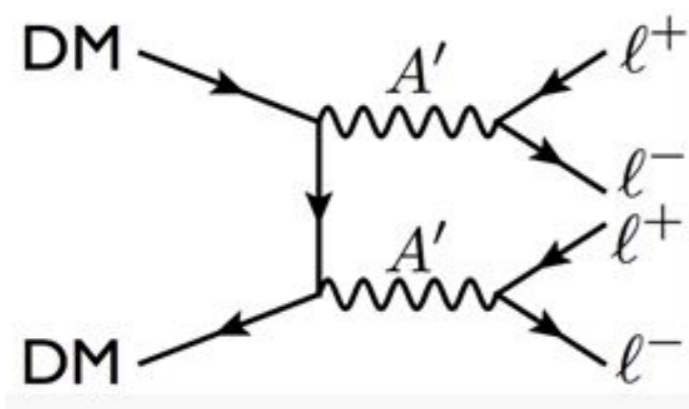
$$\mathcal{L} \supset -\frac{1}{4} F'_{\mu\nu} F'^{\mu\nu} + \frac{m_{A'}^2}{2} A'_\mu A'^\mu + \frac{\epsilon}{2 \cos \theta_W} F'_{\mu\nu} B^{\mu\nu}$$

- The mixing induces a coupling of the dark photon to the electromagnetic and weak neutral currents.

$$\mathcal{L}_{int} = -e\epsilon J_{em}^\mu A'_\mu$$

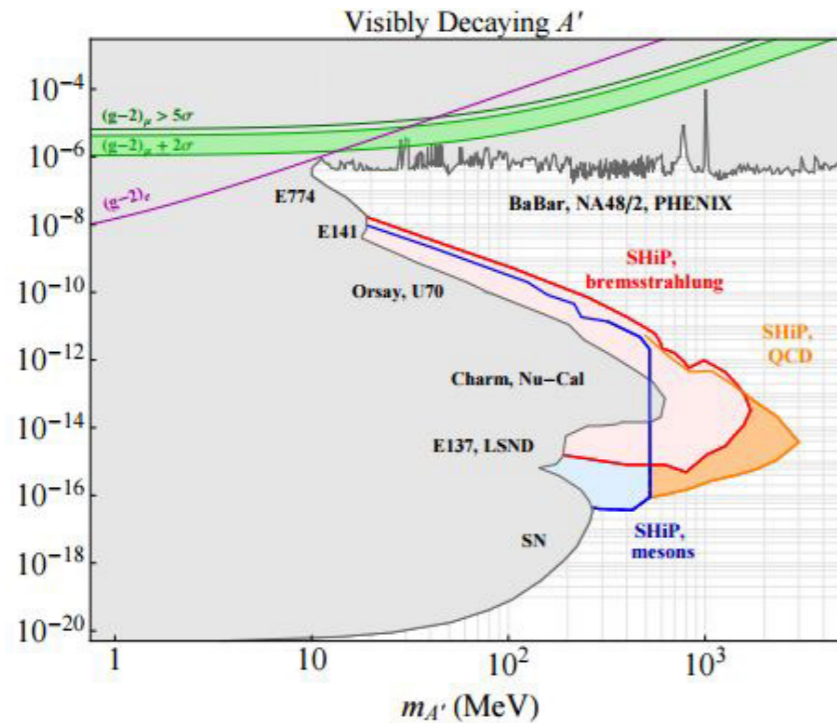
- Could help explain astrophysical data and anomalies

[Arkani-Hamed, Finkbeiner, Slatyer, Wiener, ...]

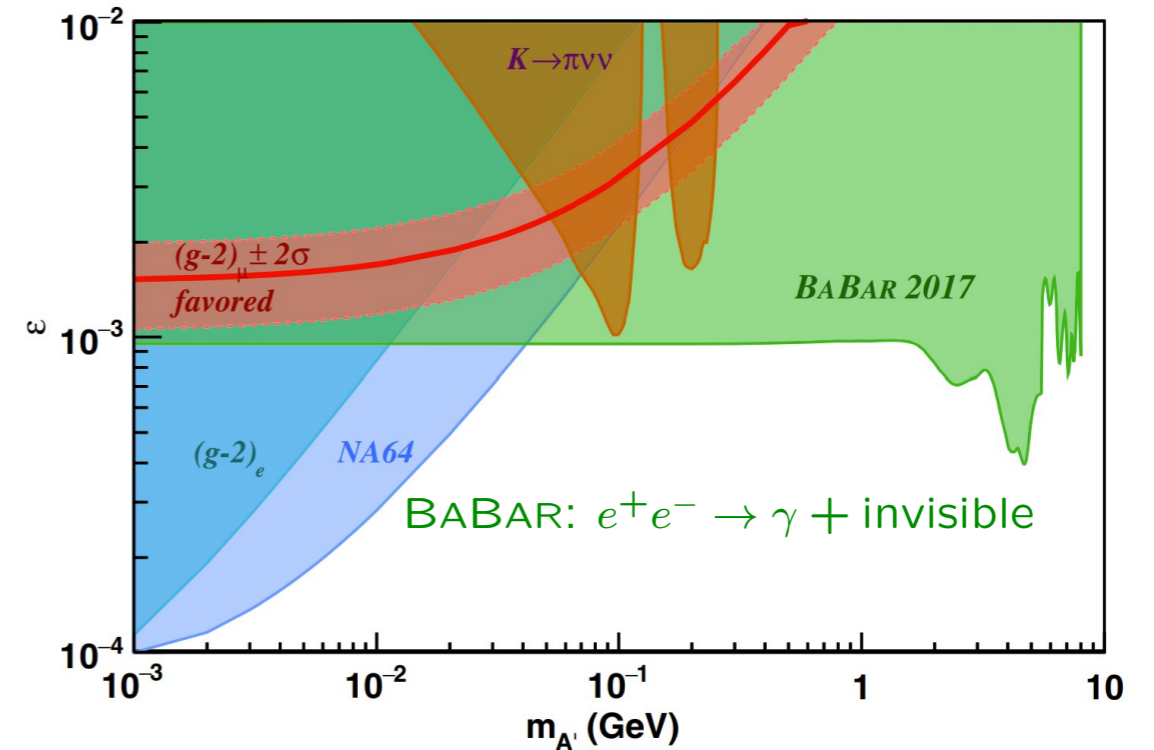


Dark Photon Scenario

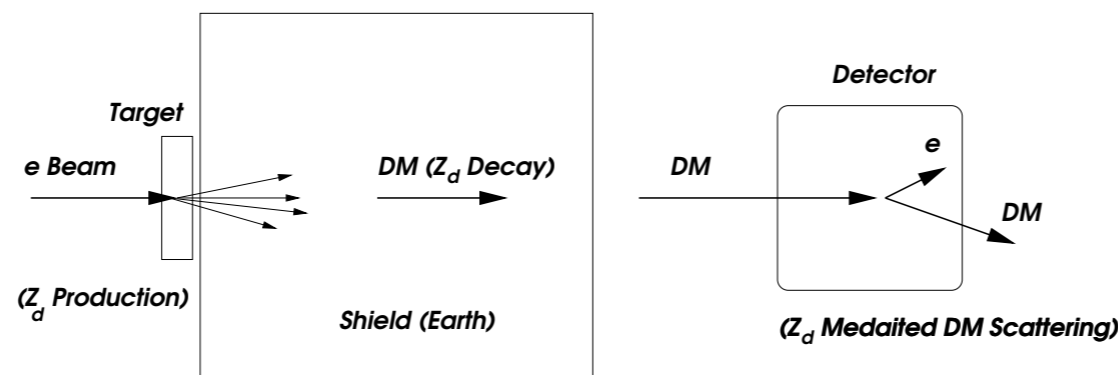
- Active experimental program to search for dark photons
 [Bjorken, Essig, Schuster, Toro; Baten, Pospelov, Ritz; Izaguirre Krnjaic, Schuster, Toro]



S. Alekhin et al., arXiv:1504.04855 [hep-ph]



- Beam Dump Experiments (see talk by Marco Spreafico)



[Bjorken, Essig, Schuster, Toro]

Dark Photon Scenario: Impact on PVES

[Thomas, Wang, Williams]

$$\mathcal{L} \supset -\frac{1}{4}F'_{\mu\nu}F'^{\mu\nu} + \frac{m_{A'}^2}{2}A'_\mu A'^\mu + \frac{\epsilon}{2\cos\theta_W}F'_{\mu\nu}B^{\mu\nu}$$

- Constraints on Dark Photon parameter space will be independent of the details of the decay branching fractions of the dark photon
- For a light dark photon, the induced coupling to the weak neutral coupling is suppressed (due to a cancellation between the kinetic and mass mixing induced couplings). [Gopalakrishna, Jung, Wells; Davoudiasl, Lee, Marciano]
- Thus, we consider a heavier dark photon for a sizable coupling to the weak neutral current and a correspondingly sizable effect in PVES. [Thomas, Wang, Williams]

Dark Photon Scenario: Impact on PVES

[Thomas, Wang, Williams]

$$\mathcal{L} \supset -\frac{1}{4}F'_{\mu\nu}F'^{\mu\nu} + \frac{m_{A'}^2}{2}A'_\mu A'^\mu + \frac{\epsilon}{2\cos\theta_W}F'_{\mu\nu}B^{\mu\nu}$$

- Constraints on Dark Photon parameter space will be independent of the details of the decay branching fractions of the dark photon
- Constraints on Dark Photon parameter space will be independent of the details of the decay branching fractions of the dark photon
- The usual PVDIS asymmetry has the form:

$$A_{\text{PV}}^{\text{DIS}} = \frac{G_F Q^2}{4\sqrt{2}(1 + Q^2/M_Z^2)\pi\alpha} \left[a_1 + \frac{1 - (1 - y)^2}{1 + (1 - y)^2} a_3 \right]$$

- Including the effects of a dark photon, we get additional terms:

$$A_{\text{PV}} = \frac{Q^2}{2\sin^2 2\theta_W (Q^2 + M_Z^2)} \left[a_1^{\gamma Z} + \frac{1 - (1 - y)^2}{1 + (1 - y)^2} a_3^{\gamma Z} \right. \\ \left. + \frac{Q^2 + M_Z^2}{Q^2 + M_{A_D}^2} \left(a_1^{\gamma A_D} + \frac{1 - (1 - y)^2}{1 + (1 - y)^2} a_3^{\gamma A_D} \right) \right],$$

Dark Photon Scenario: Impact on PVES

- Equivalent to working with the usual PVDIS formula:

$$A_{\text{PV}}^{\text{DIS}} = \frac{G_F Q^2}{4\sqrt{2}(1 + Q^2/M_Z^2)\pi\alpha} \left[a_1 + \frac{1 - (1 - y)^2}{1 + (1 - y)^2} a_3 \right]$$

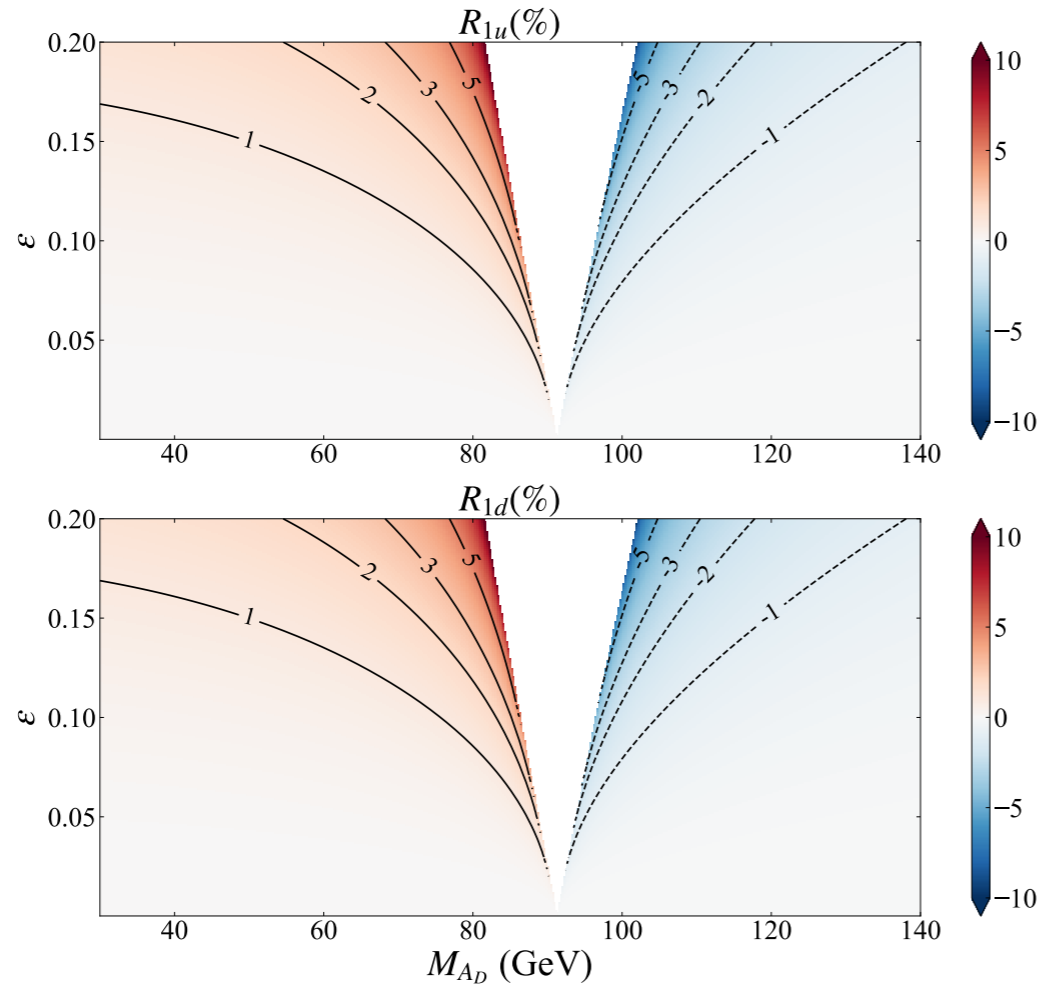
- But with shifted C_{iq} couplings:

$$C_{1q} = C_{1q}^Z + \frac{Q^2 + M_Z^2}{Q^2 + M_{A_D}^2} C_{1q}^{A_D} = C_{1q}^{\text{SM}} (1 + R_{1q})$$

$$C_{2q} = C_{2q}^Z + \frac{Q^2 + M_Z^2}{Q^2 + M_{A_D}^2} C_{2q}^{A_D} = C_{2q}^{\text{SM}} (1 + R_{2q})$$

[Thomas, Wang, Williams]

Dark Photon Scenario: Shift in C_{1q} (PREX)



$$C_{1q} = C_{1q}^Z + \frac{Q^2 + M_Z^2}{Q^2 + M_{A_D}^2} C_{1q}^{A_D} = C_{1q}^{\text{SM}} (1 + R_{1q})$$

FIG. 1. The correction factors R_{1u} and R_{1d} at $Q^2 = 0.00616 \text{ GeV}^2$, appropriate to the PREX-II experiment. The gap on the $\epsilon - M$ plane is not accessible because of “eigenmass repulsion” associated with the Z mass.

[Thomas, Wang, Williams]

Dark Photon Scenario: Shift in C_{iq} (PVDIS)

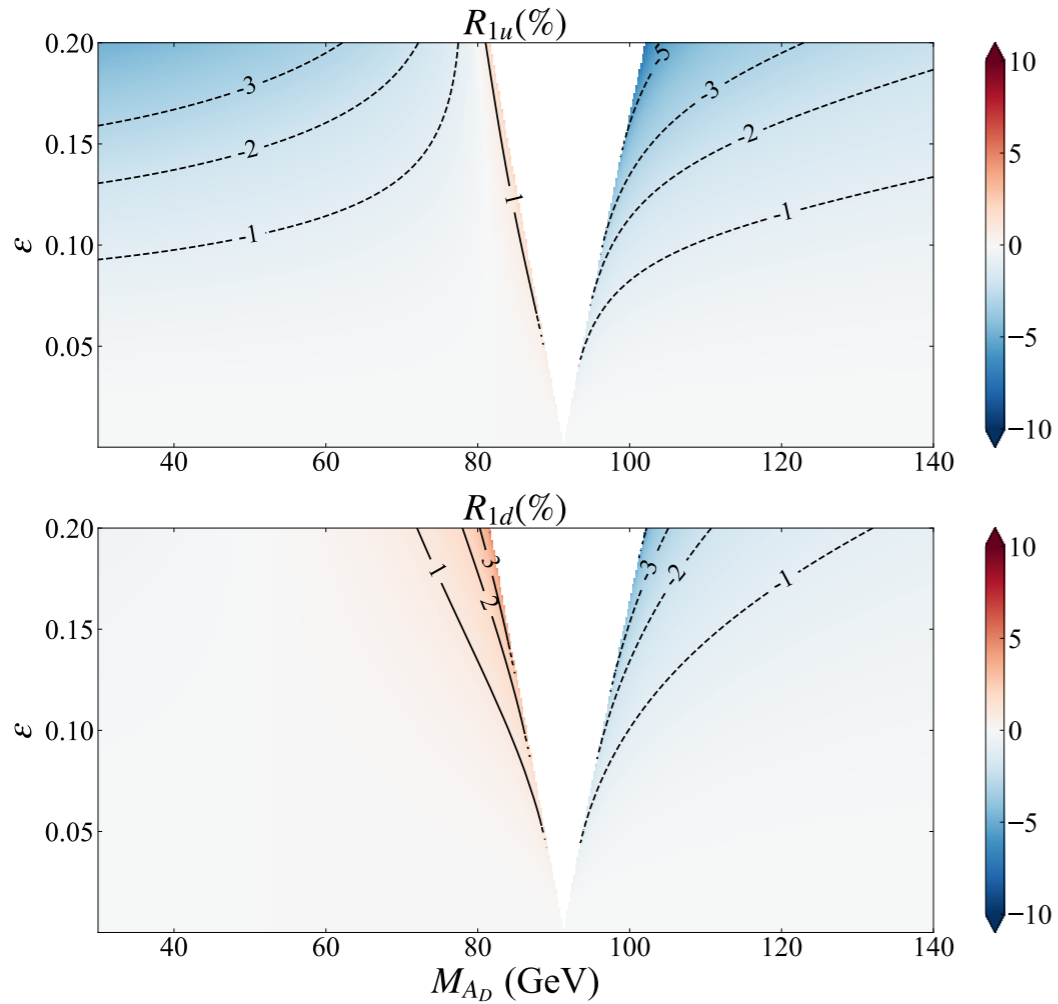


FIG. 2. The correction factors R_{1u} and R_{1d} at $Q^2 = M_Z^2$.

$$C_{1q} = C_{1q}^Z + \frac{Q^2 + M_Z^2}{Q^2 + M_{A_D}^2} C_{1q}^{A_D} = C_{1q}^{\text{SM}} (1 + R_{1q})$$

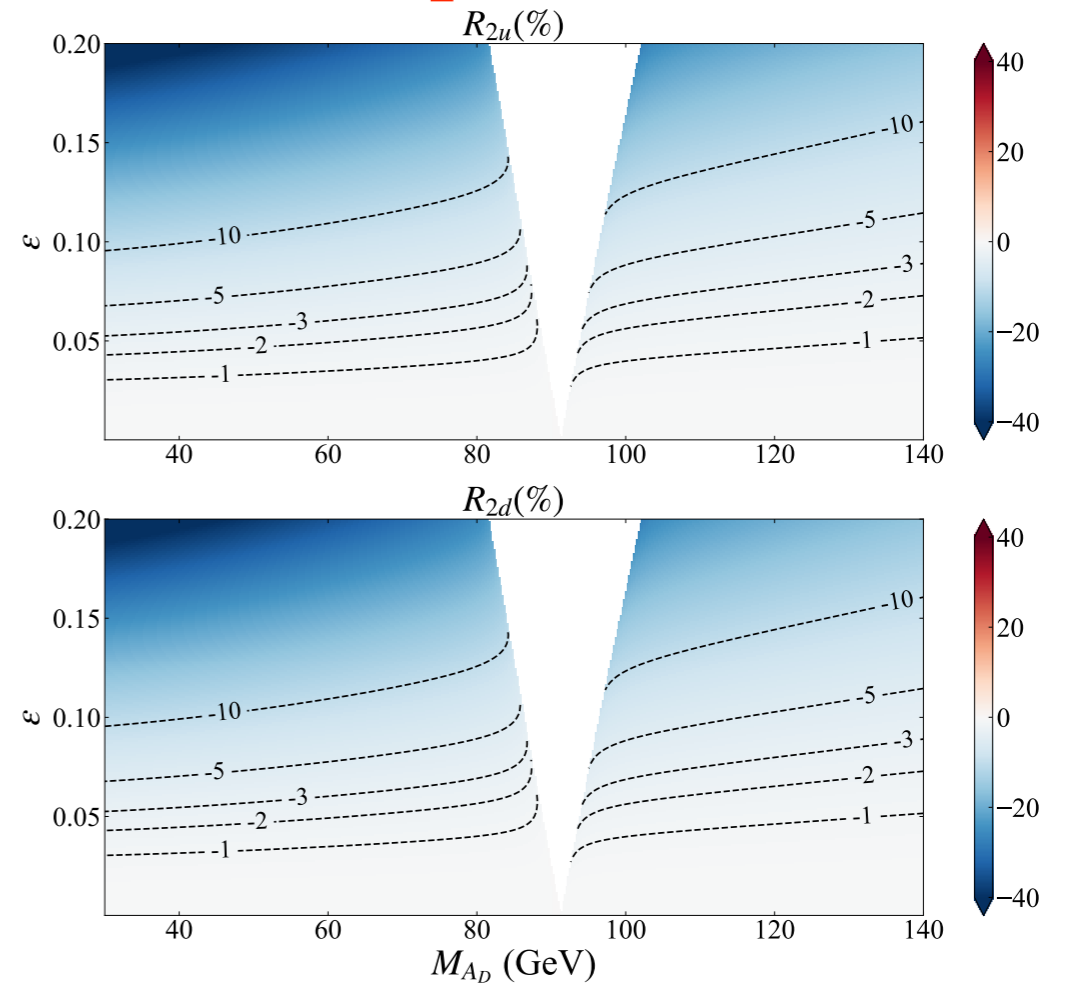
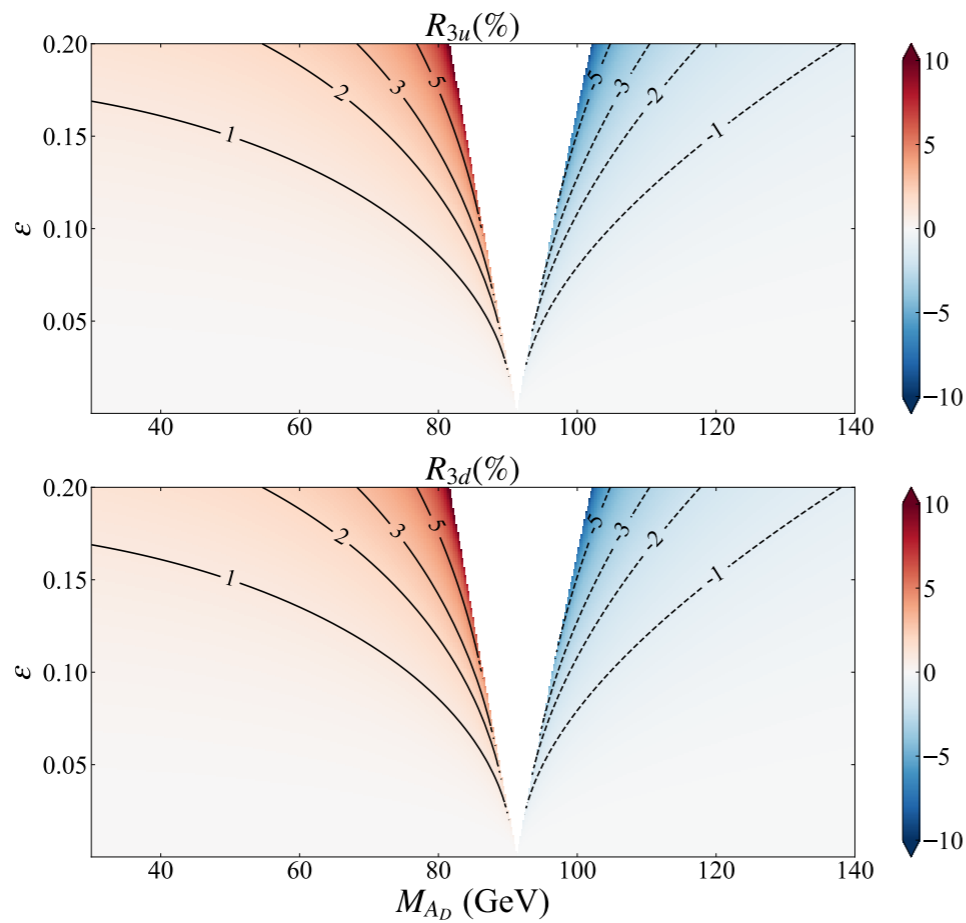


FIG. 3. The correction factors R_{2u} and R_{2d} at $Q^2 = M_Z^2$.

$$C_{2q} = C_{2q}^Z + \frac{Q^2 + M_Z^2}{Q^2 + M_{A_D}^2} C_{2q}^{A_D} = C_{2q}^{\text{SM}} (1 + R_{2q})$$

Dark Photon Scenario: Shift in C_{3q} (PVDIS)



[Thomas, Wang, Williams]

$$A_d^{e^+e^-} = -\frac{3G_F Q^2 Y}{2\sqrt{2}\pi\alpha} \frac{R_V(2g_{AA}^{eu} - g_{AA}^{ed})}{5 + 4R_C + R_S}$$

$$C_{3q} = C_{3q}^Z + \frac{Q^2 + M_Z^2}{Q^2 + M_{A_D}^2} C_{3q}^{A_D} = C_{3q}^{\text{SM}} (1 + R_{3q})$$

FIG. 4. The correction factors R_{3u} and R_{3d} at $Q^2 = 10 \text{ GeV}^2$.

Light Dark-Z Parity Violation

[Davoudiasl, Lee, Marciano]

- An interesting scenario is that of a “light” Dark-Z.

- The standard kinetic mixing scenario:

$$\mathcal{L}_{\text{gauge}} = -\frac{1}{4}B_{\mu\nu}B^{\mu\nu} + \frac{1}{2}\frac{\varepsilon}{\cos\theta_W}B_{\mu\nu}Z_d^{\mu\nu} - \frac{1}{4}Z_{d\mu\nu}Z_d^{\mu\nu}$$

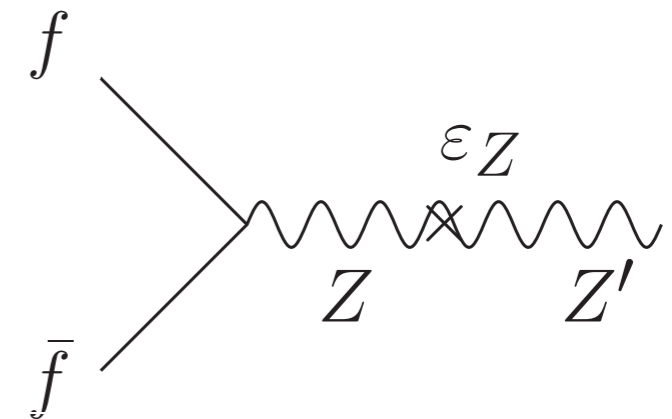
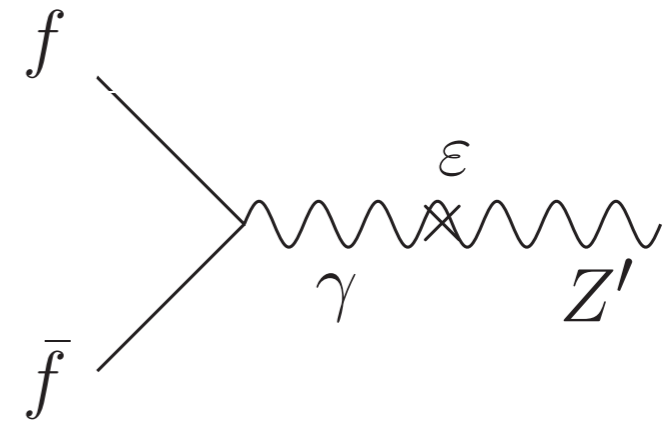
- And additional mass mixing (for example, from extended Higgs sector) ton induce sizable dark-Z coupling to the weak neutral current:

$$M_0^2 = m_Z^2 \begin{pmatrix} 1 & -\varepsilon_Z \\ -\varepsilon_Z & m_{Z_d}^2/m_Z^2 \end{pmatrix}$$

$$\varepsilon_Z = \frac{m_{Z_d}}{m_Z} \delta$$

- Dark-Z couples to the electromagnetic and neutral current coupling:

$$\mathcal{L}_{\text{int}} = \left(-e\varepsilon J_\mu^{\text{em}} - \frac{g}{2\cos\theta_W}\varepsilon_Z J_\mu^{\text{NC}} \right) Z_d^\mu$$



Light Dark-Z Parity Violation

[Davoudiasl, Lee, Marciano]

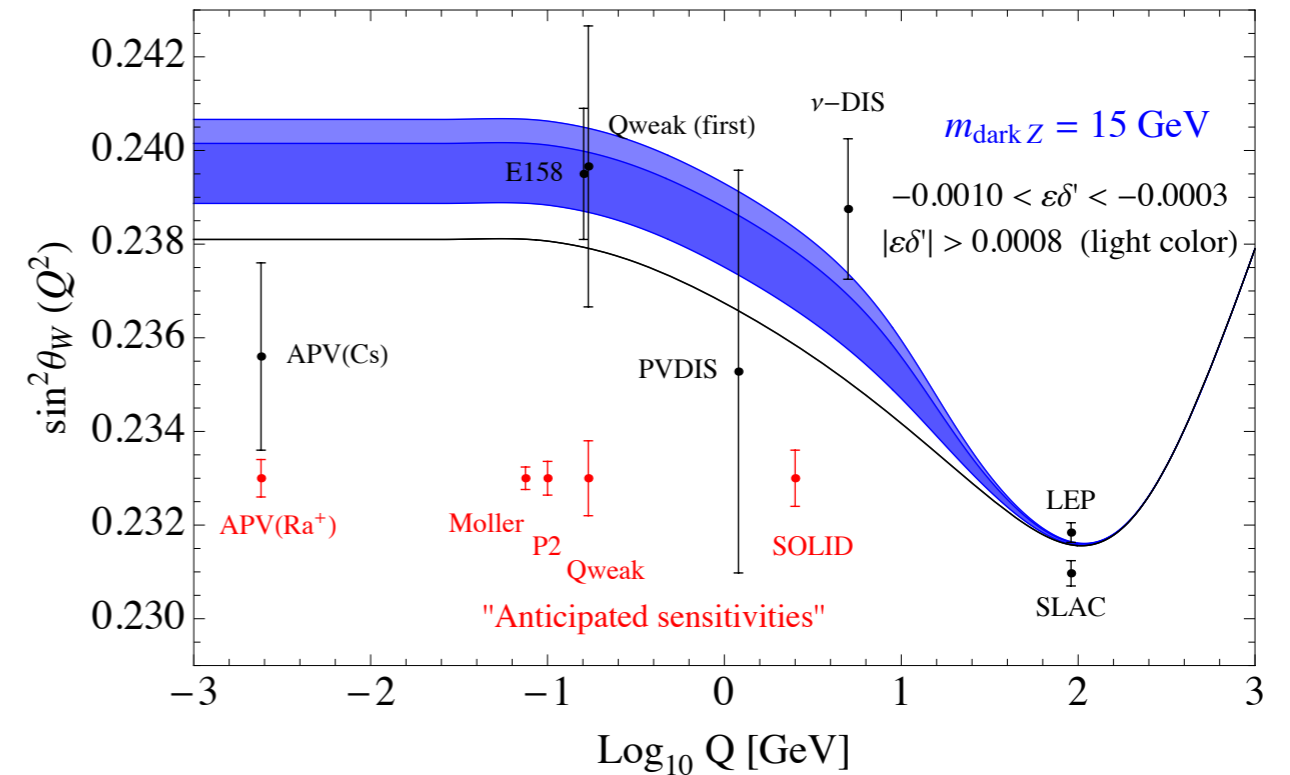
- Effective change in presence of dark-Z for parity violating asymmetries:

$$G_F \rightarrow \rho_d G_F$$

$$\sin^2 \theta_W \rightarrow \kappa_d \sin^2 \theta_W$$

$$\rho_d = 1 + \delta^2 \frac{m_{Z_d}^2}{Q^2 + m_{Z_d}^2}$$

$$\kappa_d = 1 - \frac{\varepsilon}{\varepsilon_Z} \delta^2 \frac{\cos \theta_W}{\sin \theta_W} \frac{m_{Z_d}^2}{Q^2 + m_{Z_d}^2}$$

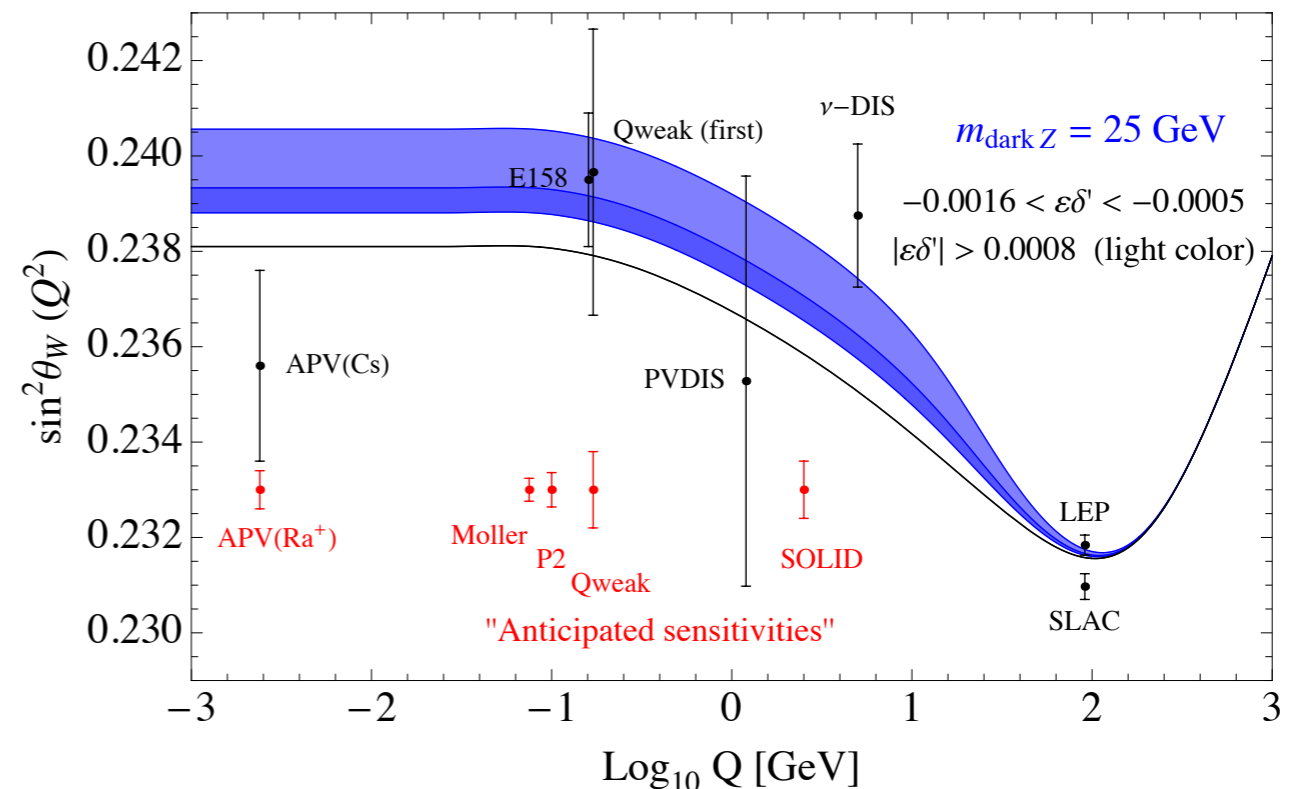


- Constraints from Higgs Decay:

$$H \rightarrow ZZ_d \rightarrow \ell_1^+ \ell_1^- \ell_2^+ \ell_2^-$$

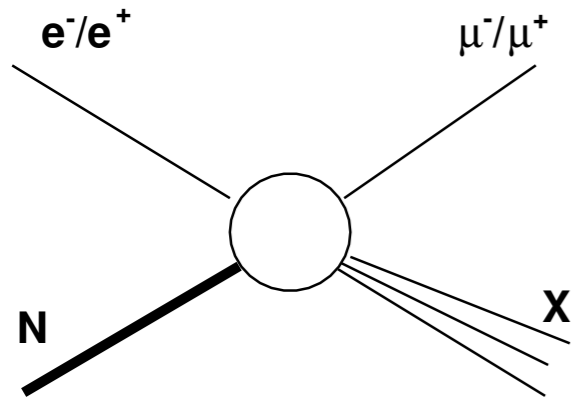
$$|\varepsilon \delta'| \lesssim 0.0008.$$

- Note that this constraint will be much weaker if the Dark Z has a larger branching fraction to the dark sector.



Charged Lepton Flavor Violation ($e^+ \rightarrow \mu^+$)

[Furletova, SM]



$$e^+ + N \rightarrow \mu^+ + X$$

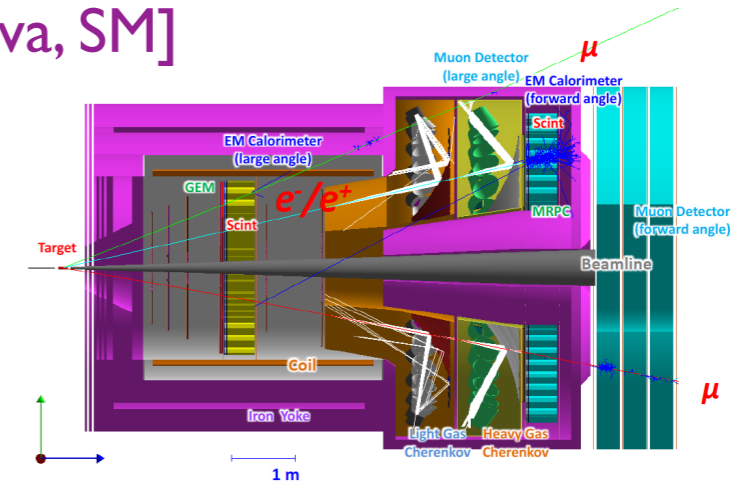


Fig. 3. The SoLID J/Ψ configuration with muon detectors [28]. Other sub-detectors are labeled.

- Low center of mass energy but high luminosity:

$$\sqrt{s} \sim 4.5 \text{ GeV}$$

$$\mathcal{L} \sim 10^{36} - 10^{39} \text{ cm}^{-2} \text{ s}^{-1}$$

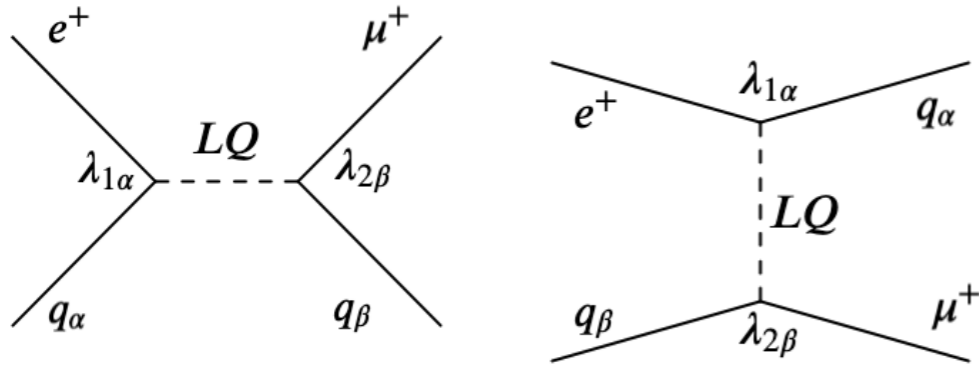
- Detectors should be equipped with muon detectors and a good tracker. Proposed SoLID spectrometer meets these requirements

- High luminosity will allow for substantial improvement over HERA limits on CLFV.

- For $\mathcal{L} \sim 10^{38} \text{ cm}^{-2} \text{ s}^{-1}$ one can expect two to three orders of magnitude improvement over HERA.

Charged Lepton Flavor Violation via Leptoquarks

□ Convenient to study CLFV in Leptoquark framework which mediates CLFV at tree-level:



$$\sigma_{F=0}^{e^+p} = \sum_{\alpha,\beta} \frac{s}{32\pi} \left[\frac{\lambda_{1\alpha}\lambda_{2\beta}}{M_{LQ}^2} \right]^2 \int dx \int dy \left\{ x q_\alpha(x, xs) f(y) + x \bar{q}_\beta(x, -u) g(y) \right\}$$

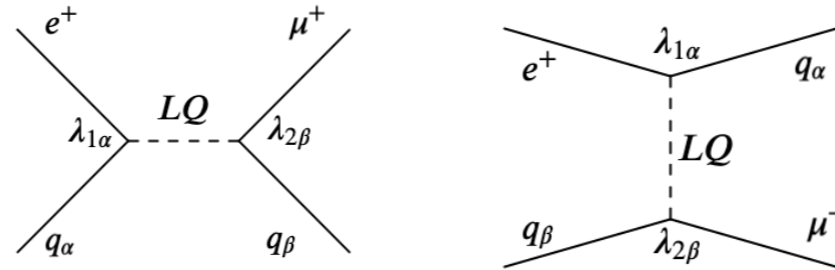
$$\sigma_{|F|=2}^{e^+p} = \sum_{\alpha,\beta} \frac{s}{32\pi} \left[\frac{\lambda_{1\alpha}\lambda_{2\beta}}{M_{LQ}^2} \right]^2 \int dx \int dy \left\{ x \bar{q}_\alpha(x, xs) f(y) + q_\beta(x, -u) g(y) \right\}$$

□ 14 LQ states. Positron beam can help disentangle F=0 and |F|=2 LQ states. Polarized beams can help distinguish between left-handed and right-handed LQs.

Type	J	F	Q	ep dominant process	Coupling	Branching ratio β_ℓ	Type	J	F	Q	ep dominant process	Coupling	Branching ratio β_ℓ
S_0^L	0	2	-1/3	$e_L^- u_L \rightarrow \begin{cases} \ell^- u \\ \nu_\ell d \end{cases}$	$\begin{matrix} \lambda_L \\ -\lambda_L \end{matrix}$	$\begin{matrix} 1/2 \\ 1/2 \end{matrix}$	V_0^L	1	0	+2/3	$e_R^+ d_L \rightarrow \begin{cases} \ell^+ d \\ \bar{\nu}_\ell u \end{cases}$	$\begin{matrix} \lambda_L \\ \lambda_L \end{matrix}$	$\begin{matrix} 1/2 \\ 1/2 \end{matrix}$
S_0^R	0	2	-1/3	$e_R^- u_R \rightarrow \ell^- u$	λ_R	1	V_0^R	1	0	+2/3	$e_L^+ d_R \rightarrow \ell^+ d$	λ_R	1
\tilde{S}_0^R	0	2	-4/3	$e_R^- d_R \rightarrow \ell^- d$	λ_R	1	\tilde{V}_0^R	1	0	+5/3	$e_L^+ u_R \rightarrow \ell^+ u$	λ_R	1
S_1^L	0	2	-1/3	$e_L^- u_L \rightarrow \begin{cases} \ell^- u \\ \nu_\ell d \end{cases}$	$\begin{matrix} -\lambda_L \\ -\lambda_L \end{matrix}$	$\begin{matrix} 1/2 \\ 1/2 \end{matrix}$	V_1^L	1	0	+2/3	$e_R^+ d_L \rightarrow \begin{cases} \ell^+ d \\ \bar{\nu}_\ell u \end{cases}$	$\begin{matrix} -\lambda_L \\ \lambda_L \end{matrix}$	$\begin{matrix} 1/2 \\ 1/2 \end{matrix}$
			-4/3	$e_L^- d_L \rightarrow \ell^- d$	$-\sqrt{2}\lambda_L$	1				+5/3	$e_R^+ u_L \rightarrow \ell^+ u$	$\sqrt{2}\lambda_L$	1
$V_{1/2}^L$	1	2	-4/3	$e_L^- d_R \rightarrow \ell^- d$	λ_L	1	$\tilde{S}_{1/2}^L$	0	0	+5/3	$e_R^+ u_R \rightarrow \ell^+ u$	λ_L	1
$V_{1/2}^R$	1	2	-1/3	$e_R^- u_L \rightarrow \ell^- u$	λ_R	1	$S_{1/2}^R$	0	0	+2/3	$e_L^+ d_L \rightarrow \ell^+ d$	$-\lambda_R$	1
			-4/3	$e_R^- d_L \rightarrow \ell^- d$	λ_R	1				+5/3	$e_L^+ u_L \rightarrow \ell^+ u$	λ_R	1
$\tilde{V}_{1/2}^L$	1	2	-1/3	$e_L^- u_R \rightarrow \ell^- u$	λ_L	1	$\tilde{S}_{1/2}^R$	0	0	+2/3	$e_R^+ d_R \rightarrow \ell^+ d$	λ_L	1

□ HERA put limits on the ratio of the product LQ couplings and the LQ mass squared:

$$\chi_{\alpha\beta} \equiv \frac{\lambda_{1\alpha}\lambda_{2\beta}}{M_{LQ}^2}$$



□ Define “z” such that z=1 corresponds to the HERA limit and z < 1 an improvement over the HERA limit:

$$z \equiv \frac{\chi_{\alpha\beta}}{\chi_{\alpha\beta}^{\text{HERA}}}$$

[Furletova, SM]

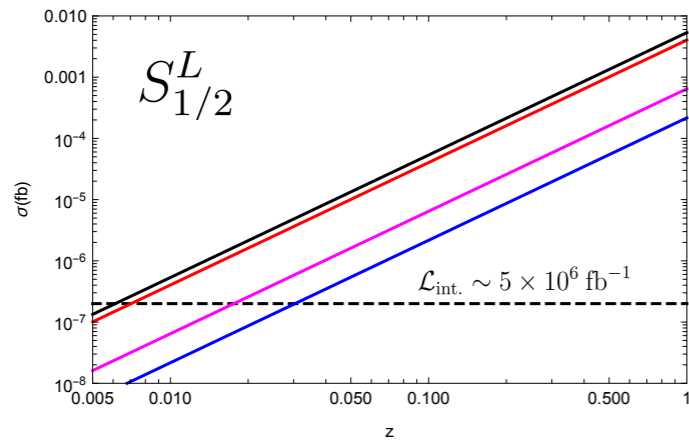


Fig. 5. The cross section for $e^+N \rightarrow \mu^+X$ with center of mass energy $\sqrt{s} = 4.5$ GeV, via exchange of the F=0 scalar LQ, $S_{1/2}^L$, as a function of the ratio z defined in Eq. (9). The red, black, magenta, and blue solid lines correspond to the choices $(\alpha, \beta) = \{11, 12, 21, 22\}$ in Eq. (6) with all other terms set to zero. An integrated luminosity of $\mathcal{L} \sim 5 \times 10^6 \text{ fb}^{-1}$ will allow sensitivity to cross sections as small as $\sigma \sim 0.2 \times 10^{-6} \text{ fb}$ (horizontal dashed line).

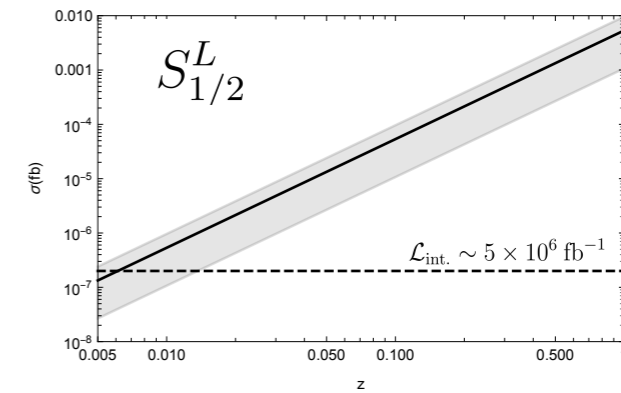


Fig. 6. The positron beam polarization dependence of cross section for $e^+N \rightarrow \mu^+X$ with center of mass energy $\sqrt{s} = 4.5$ GeV, via exchange of the F=0 scalar LQ, $S_{1/2}^L$, as a function of the ratio z defined in Eq. (9). The solid black line corresponds to the cross section for an unpolarized positron beam ($P_e = 0$). The gray band corresponds to the linear variation of the cross section with beam polarization, as shown in Eq. (11). The size of the band corresponds to a variation of the beam polarization between [-80%,80%].

Conclusions

- PVDIS at JLAB can provide unique and complementary information to constrain new physics
- It can provide input for the global SMEFT analysis by lifting flat directions and disentangling dim-6 and dim-8 operators
- Can constrain the parameter space of Dark photons/Z
- Additionally, could improve on HERA limits for Charged Lepton Violation ($e \rightarrow \mu$)